The Geological Society of America Bulletin

The Laurentian record of Neoproterozoic glaciation, tectonism, and eukaryotic evolution in Death Valley, California

--Manuscript Draft--

Manuscript Number:	B30789R2
Full Title:	The Laurentian record of Neoproterozoic glaciation, tectonism, and eukaryotic evolution in Death Valley, California
Short Title:	Neoproterozoic glaciation, tectonism, and eukaryotic evolution in Death Valley
Article Type:	Article
Keywords:	Sturtian; Kingston Peak; strontium; Cryogenian; Microfossils
Corresponding Author:	Francis Alexander Macdonald, Ph.D. Harvard University Cambridge, MA UNITED STATES
Corresponding Author's Institution:	Harvard University
First Author:	Francis Alexander Macdonald, Ph.D.
Order of Authors:	Francis Alexander Macdonald, Ph.D.
	Anthony R. Prave
	Ryan Petterson
	Emily F. Smith
	Sara B. Pruss
	Kaylyn Oates
	Felix Waechter
	Dylan Trotzuk
	Anthony Fallick
Abstract:	Neoproterozoic strata in Death Valley, California contain eukaryotic microfossils and glacial deposits that have been used to assess the severity of putative Snowball Earth events and the biological response to extreme environmental change. These successions also contain evidence for syn-sedimentary faulting that has been related to the rifting of Rodinia, and in turn the tectonic context of the onset of Snowball Earth. These interpretations hinge on local geological relationships and both regional and global stratigraphic correlations. Here we present new geological mapping, measured stratigraphic sections, carbon and strontium isotope chemostratigraphy, and micropaleontology from the Neoproterozoic glacial deposits and bounding strata in Death Valley. These new data enable us to refine regional correlations both across Death Valley and throughout Laurentia, and construct a new age model for glaciogenic strata and microfossil assemblages. Particularly, our remapping of the Kingston Peak Formation in the Saddle Peak Hills and near the type locality shows for the first time that glacial deposits of both the Marinoan and Sturtian glaciations can be distinguished in southeastern Death Valley, and that beds containing vase-shaped microfossils are slump blocks derived from the underlying strata. These slump blocks are associated with multiple overlapping unconformities that developed during syn-sedimentary faulting, which is a common feature of Cyrogenian strata along the margin of Laurentia from California to Alaska. With these data, we conclude that all of the microfossils that have been described to date in Neoproterozoic strata of Death Valley predate the glaciations and do not bear on the severity, extent or duration of Neoproterozoic Snowball Earth events.
Suggested Reviewers:	Karl E. Karlstrom kek1@unm.edu Dr. Karlstrom is an expert on the Precambrian geology of the western US.
	Clark Burchfiel

	bcburch@mit.edu Dr. Burchfiel is an expert on the Geology of W. US and previously mapped some of the localities that we describe in the Kingston Range
	Carol Dehler Carol.Dehler@usu.edu Dr. Dehler has been working on equivalent rocks in the Grand Canyon, Uinta Mountains, and recently in Death Valley as well on the geochronology, stratigraphy, and paleontology.
	David Evans dai.evans@yale.edu Dr. Evans has worked extensively on Rodinia paleogeography and on the extent of Neoproterozoic glaciations
	Susanna Porter porter@geol.ucsb.edu Susanna is an expert on Neoproterozoic microfossils
	Brian Wernicke brian@gps.caltech.edu Brian is an expert on Death Valley tectonics and Neoproterozoic glaciation
	Mathew Hurtgen matt@earth.northwestern.edu Matt is an expert in Neoproterozoic geochemistry and has worked previously in Death Valley
	Graham Shields g.shields@ucl.ac.uk Graham is an expert in chemostratigrpahy and has worked extensively on the Sr cycle
	Galen Halverson galen.halverson@mcgill.ca Dr. Halverson is an expert in Neoproterozoic stratigraphy and geochemistry and has worked extensively to construct Sr isotope composite curves
Opposed Reviewers:	Frank Corsetti Our work directly contradicts Dr. Corsetti's previous work and demonstrates many of his conclusions were based on sampling without mapping--I'm affraid it will be very difficult for Dr. Corsetti to be impartial.
	Martin Kennedy Dr. Kennedy is outright hostile towards chemo-stratigraphy and any suggestion of Snowball Earth--eventhough the focus of this paper is really map relationships, it will be hard for Dr. Kennedy to be impartial to anyone who has worked with Paul Hoffman....
Response to Reviewers:	

Cover Letter

Click here to download Cover Letter: Macdonald_coverletter_revisions_round2.docx

The Laurentian record of Neoproterozoic glaciation, tectonism, and eukaryotic evolution in Death Valley, California

Francis A. Macdonald[1*], Anthony R. Prave[2], Ryan Petterson[3], Emily F. Smith[1], Sara B. Pruss[4], Kaylyn Oates[4], Felix Waechter[1], Dylan Trotzuk[1], Anthony E. Fallick[5]

[1] *Department of Earth and Planetary Sciences, Harvard University, Cambridge, MA 02138*
[2] *Department of Earth Science, University of St. Andrews, St. Andrews, KY16 9AL, Scotland/UK*
[3] *School of Earth Sciences, The University of Queensland, Brisbane, QLD 4023, Australia*
[4] *Department of Geosciences, Smith College, Northampton, MA 01063*
[5] *Scottish Universities Environmental Research Centre, East Kilbride, G75 0QF, Scotland/UK*
[*] *Send correspondence to: fmacdon@fas.harvard.edu*

ABSTRACT

Neoproterozoic strata in Death Valley, California contain eukaryotic microfossils and glacial deposits that have been used to assess the severity of putative Snowball Earth events and the biological response to extreme environmental change. These successions also contain evidence for syn-sedimentary faulting that has been related to the rifting of Rodinia, and in turn the tectonic context of the onset of Snowball Earth. These interpretations hinge on local geological relationships and both regional and global stratigraphic correlations. Here we present new geological mapping, measured stratigraphic sections, carbon and strontium isotope chemostratigraphy, and micropaleontology from the Neoproterozoic glacial deposits and bounding strata in Death Valley. These new data enable us to refine regional correlations both across Death Valley and throughout Laurentia, and construct a new age model for glaciogenic strata and microfossil assemblages. Particularly, our remapping of the Kingston Peak Formation in the Saddle Peak Hills and near the type locality shows for the first time that glacial deposits of both the Marinoan and Sturtian glaciations can be distinguished in southeastern Death Valley, and that beds containing vase-shaped microfossils are slump blocks derived from the underlying strata. These slump blocks are associated with multiple overlapping unconformities that developed during syn-sedimentary faulting, which is a common feature of Cyrogenian strata along the margin of Laurentia from California to Alaska. With these data, we conclude that all of the microfossils that have been described to date in Neoproterozoic strata of Death Valley predate the glaciations and do not bear on the severity, extent or duration of Neoproterozoic Snowball Earth events.

INTRODUCTION

The Neoproterozoic Era (1000-542 Ma) witnessed a major diversification of eukaryotes, including the origin of animals (Knoll et al., 2006), and extreme swings in climate, including putative Snowball Earth events (Hoffman et al., 1998; Kirschvink, 1992). The apparent coincidence between Neoproterozoic glacial events and the appearance of animals in the fossil record (Erwin et al., 2011; Love et al., 2009; Macdonald et al., 2010b; Peterson et al., 2008; Yin et al., 2007) has fueled speculation concerning the relationships between extreme climate change and eukaryotic evolution (Boyle et al., 2007; Costas et al., 2008; Hoffman and Schrag, 2002). Alternatively, the presence of photosynthetic autotrophs and heterotrophs before, and their survival through, Neoproterozoic glaciations (Corsetti et al., 2003; Corsetti et al., 2006; Olcott et al., 2005; Porter and Knoll, 2000) has been argued to preclude a Snowball Earth scenario (Corsetti, 2009; Moczydlowska, 2008; Runnegar, 2000). These interpretations are only as good as the records on which they are based. Although the microfossil record from strata deposited during the Cryogenian[1] glacial interlude has increased dramatically with discoveries from Namibia (Bosak et al., 2011a; Bosak et al., 2012; Brain et al., 2012; Pruss et al., 2010) and Mongolia (Bosak et al., 2011b), attempts at integrating Cryogenian fossil records globally and assessing the biological response to Neoproterozoic glaciation have been frustrated by the dearth of geochronological constraints, along with uncertainties in stratigraphic correlations between different fossil localities.

[1] The Cryogenian Period is formally defined from 850-635 Ma. Herein we follow the recommendation of the IGCP 512 Neoproterozoic stratigraphic sub-commission, which defines the base of the Cryogenian at the base of the oldest Neoproterozoic glacial deposit from a global glaciation. While there is still controversy over the possibility of pre-Sturtian, ca. 750 Ma glaciations, we assume that these deposits are not global and take the onset of the Sturtian glaciation at 717 Ma as the base of the Cryogenian Period.

Ease of accessibility and spectacular exposure has made the Pahrump Group of Death Valley, California (Fig. 1), an iconic record of Neoproterozoic environmental change. Distinct early Cryogenian “Sturtian” (ca. 717-662 Ma; Bowring et al., 2007; Macdonald et al., 2010b; Zhou et al., 2004) glacial deposits and late Cryogenian “Marinoan” (ca. 635 Ma; Condon et al., 2005; Hoffmann et al., 2004) glacial deposits are present in the Kingston Peak Formation on the west side of Death Valley, in the Panamint Mountains (Miller, 1985; Petterson et al., 2011; Prave, 1999). However, in southeastern Death Valley, it has remained unclear if glacial deposits of the Kingston Peak Formation are Sturtian or Marinoan in age (Mrofka and Kennedy, 2011; Prave, 1999). Conversely, in southeastern Death Valley, vase-shaped microfossils (VSMs), filamentous organisms, possible algae, and cyanobacteria are present in the Pahrump Group (Corsetti et al., 2003; Licari, 1978; Pierce and Cloud, 1979), whereas Neoproterozoic microfossils have not been identified on the west side of Death Valley. These paleontological finds include a putative syn-glacial biota in the “oncolite bed” of the Kingston Peak Formation (Corsetti et al., 2003), but because of stratigraphic uncertainties and structural complexity in southeastern Death Valley (Walker et al., 1986), the age of these microfossil assemblages has remained unclear (Hoffman and Maloof, 2003; Macdonald et al., 2010b). Stratigraphic relationships have been complicated by syn-depositional tectonism, which has left the succession with multiple overlapping unconformities, many redeposited beds, and large lateral facies changes. Here we present new geological mapping, measured stratigraphic sections, carbon and strontium isotope chemostratigraphy, and microfossil discoveries from key localities in southeastern Death Valley (Fig. 1). These data allow us to unify Neoproterozoic records across the valley and beyond, and reassess the stratigraphic relationship between global glaciation and biological turnover.

GEOLOGICAL SETTING

Exposures in the Death Valley region of southern California (Fig. 1) record the geological evolution of the southwestern margin of Laurentia. The oldest rocks in the region are ca. 1.76 Ga granitic gneisses of the Mojave crustal province (Barth et al., 2000; Strickland et al., 2012; Wasserburg et al., 1959), which are intruded by ca. 1.4 Ga porphyritic quartz monzonite (Labotka et al., 1980). Unconformably overlying those basement rocks, is the Pahrump Group, a 1.5-4 km thick mixed carbonate and siliciclastic succession exposed across southeastern Death Valley and the Panamint Mountains (Hazzard, 1937; Hewett, 1940, 1956; Noble, 1934; Wright et al., 1974). Upwards, it consists of the Crystal Spring Formation (here differentiated into the upper and lower Crystal Spring Formation), the Beck Spring Dolomite, and the Kingston Peak Formation (Fig. 2). The lower portions of the Crystal Spring Formation are intruded by 1.08 Ga diabase sills (Heaman and Grotzinger, 1992). A minimum age for the Pahrump Group is provided by the overlying Noonday Formation (Hazzard, 1937; Hewett, 1956; Noble, 1934; Wright et al., 1974), the lowest member of which has been identified as a basal Ediacaran cap dolostone (Petterson et al., 2011), dated globally at 635 Ma (Condon et al., 2005; Hoffmann et al., 2004). The Noonday Formation is succeeded by the Johnnie Formation, Stirling Quartzite, and the early Cambrian Wood Canyon Formation, which contains the Precambrian-Cambrian boundary (Corsetti and Hagadorn, 2000).

Following multiple episodes of late Neoproterozoic extension (Prave, 1999;

Stewart, 1975), and subsequent Cambrian passive-margin development (Armin and Mayer, 1983; Stewart, 1970), the region experienced Permian contraction and magmatism (Snow et al., 1991). This was followed by the Mesozoic Cordilleran orogeny (Burchfiel et al., 1992; Burchfiel et al., 1970; Snow and Wernicke, 1990), and Neogene extension accommodated by break-away detachment faults (Snow and Wernicke, 2000; Wernicke et al., 1988; Wright, 1976) with associated felsic and mafic intrusions (Calzia and Ramo, 2000; Fleck, 1970; Wright et al., 1991).

Stratigraphy of the Pahrump Group

Crystal Spring Formation

The Pahrump Group begins with the Crystal Spring Formation, which is 300-1000 m thick and rests nonconformably on Mesoproterozoic granitic to amphibolitic gneissic basement (Roberts, 1982; Wright, 1968). Above this surface is a variably developed basal conglomerate (interestingly, this unit is dominated by light-colored meta-quartzite clasts rather than gneissic ones) that is overlain by purple to violet quartzite and shale followed by a thick (many tens of meters) stromatolitic dolostone and then a cherty mudstone and fine-grained quartzite unit (Roberts, 1982). The 1.08 Ga diabase sills (Heaman and Grotzinger, 1992) intrude these strata, generating hornfels and talc (Wright, 1968). The lower Crystal Spring Formation is unconformably overlain by the upper Crystal Spring Formation, which is a mixed siliciclastic-carbonate succession that is ~100-650 m thick, and is not intruded by the diabase.

Beck Spring Dolomite

The contact between the upper Crystal Spring Formation and the Beck Spring Dolomite is transitional and conformable (Roberts, 1982), and is placed at the base of the first well-defined, meter-scale carbonate parasequence, where the succession transitions to carbonate-dominated deposition. The Beck Spring Dolomite is 100-400 m thick, and consists predominantly of blue-grey dolostone with abundant microbialite and oolitic packstone, occasional micrite with molar tooth structure, and minor siliciclastic interbeds (Gutstadt, 1968; Marian and Osborne, 1992).

Kingston Peak Formation

The Kingston Peak Formation is lithologically diverse, characterized by glacigenic diamictites, but also including carbonates and other non-glacigenic siliciclastic rocks. The Kingston Peak Formation has proven to be problematic with regard to establishing a regional stratigraphic framework. This is due in part to the presence of only one widespread diamictite unit in southeastern Death Valley (KP2) whereas in the Panamint Mountains there are two (Surprise and Wildrose diamictites), including a well-developed non-glacial stratigraphy between these glaciogenic intervals that is lacking in southeastern Death Valley. In the Panamint Mountains, the Kingston Peak Formation has been divided into the Limekiln Spring, Surprise, Sourdough, Middle Park, Argenta, Mountain Girl, Thorndike (also referred to as the 'unnamed' limestone), and Wildrose members (Miller, 1985; Petterson et al., 2011). The Surprise and Wildrose members have been suggested to represent Sturtian and Marinoan glacial deposits, respectively (Petterson et al., 2011; Prave, 1999). In contrast, in southeastern Death Valley the formation consists of three informal mapable units, KP1-2-3, a locally developed fourth unit, KP4 (Prave, 1999; Wright, 1954), and an enigmatic limestone unit, the Virgin Spring Limestone (Tucker, 1986), which is variably present at the contact between KP1 and KP2. Some studies have further divided the Kingston Peak Formation into northern and southern facies belts as a function of clast composition (Mrofka and Kennedy, 2011; Troxel, 1966, 1967). Here we use the KP1-KP4 nomenclature, rather than the northern and southern facies, and further subdivide KP3 into several mappable units.

Unit KP1 is as much as 250 m thick and consists predominantly of thinly-bedded (1-10 cm-thick beds), mostly flat-laminated (ripple cross-lamination is present locally) to graded, fine-grained sandstone and shale with minor nodular dolostone.

The Virgin Spring Limestone sharply overlies KP1, and has previously been described in the Black Mountains and Southern Ibex Hills (Fig. 1) as a <20 m thick, fine-laminated limestone (Tucker, 1986). In the Kingston Range and Alexander Hills, the Virgin Spring Limestone is missing and KP2 rests sharply on KP1.

Unit KP2 is a massive, poorly bedded diamictite that is 50 to 370 m thick. Clasts range in size from pebbles to boulders and consist of gneissic rocks derived from the basement, and quartzite and dolostone from the underlying Crystal Spring Formation and Beck Spring Dolomite; glacially striated clasts are present but rare (Miller et al., 1988). The matrix varies from brown colored where carbonate-rich to greenish-black, where dominated by mud- and sand-sized siliciclastics. The contact at the top of KP2 with the overlying KP3 rocks is variable; in some places it is sharp and in others gradational.

Unit KP3 has a clast composition similar to KP2 but is typically dominated by clasts derived from the Beck Spring Dolomite and the Crystal Spring Formation. KP3 consists of several interbedded lithologies: meters-thick, matrix- and clast-supported sedimentary breccias and conglomerates, centimeter- to meter-thick, fine- to very coarse-grained graded sandstone beds, and shale. KP3 varies enormously in its development, ranging in thickness from as little as a few tens of meters to as much as several kilometers; it is green to reddish-brown in color and contains rare beds of iron formation. An oncolite-bearing dolostone layer was previously mapped as a laterally continuous marker bed in the KP3 (Calzia, 1990; Wright, 1974). The "oncolite bed" consists of large, partially silicified ooids and pebble- to cobble-sized oncoids in light-grey dolostone, and contains a rich microfossil assemblage (Corsetti et al., 2003). KP3 also commonly contains olistoliths derived from the underlying units that range from car-sized blocks to having length dimensions of more than a kilometer (Troxel, 1966).

In southeastern Death Valley, additional lenses of massive diamictite, unit KP4, overlies stratified diamictite of KP3. This massive diamictite and the overlying Noonday Formation rest unconfomably on all the underlying strata and basement (Prave, 1999; Wright, 1974).

METHODS

Tectonostratigraphic Units

Prave (1999) developed a correlation scheme for the Pahrump Group through geological mapping and the identification of unconformity-bound tectonostratigraphic units. Here we refine this framework (Fig. 2) by providing new observations from across the Death Valley outcrop belt. We focused our efforts on key exposures of the Kingston Peak Formation in the Black Mountains (Virgin Spring Wash), Kingston Range, Southern Ibex Hills (Saratoga Springs), and the Saddle Peak Hills (Fig. 1), including detailed mapping of the latter (Fig. 3). Although formational contacts rarely coincide with the surfaces defining the tectonostratigraphic units, we retain pre-existing nomenclature as much as possible for consistency with previously published literature.

Stratigraphic correlations of the map units that bound the Kingston Peak Formation in Death Valley region are relatively straightforward (i.e. the Beck Spring Dolomite and the Noonday Formation); however, correlation of map units within Kingston Peak strata has proven to be frustrating. In large part this is due to syn-depositional tectonism resulting in multiple overlapping unconformities and large lateral facies and thickness changes. Thus, to avoid forcing layer-cake-like, lithostratigraphically-based correlations onto a succession of rocks in which units are laterally discontinuous and/or missing, we have used the unconformity surfaces bounding our newly refined tectonostratigraphic units as a means of constructing a pan-Death-Valley Pahrump Group correlation scheme (Fig. 2), with the aim to extend these Neoproterozoic tectonostratigraphic units along the western margin of Laurentia.

Chemostratigraphy

To test regional and global correlations, we sampled carbonates in measured stratigraphic sections and constructed detailed carbon ($\delta^{13}C$) and oxygen ($\delta^{18}O$) isotopic profiles through the Beck Spring Dolomite and the Virgin Spring Limestone in the Black Mountains, Kingston Range, Saddle Peak Hills, and Southern Ibex Hills (Fig. 1). In addition, strontium isotope ($^{87}Sr/^{86}Sr$) data were obtained for the Virgin Spring Limestone.

New carbonate $\delta^{13}C$ and $\delta^{18}O$ measurements were obtained on 290 samples (see data repository Tables S1 and S2). Samples were micro-drilled along individual laminations (where visible) to obtain 5 to 50 mg of powder; areas of veining, fracturing, and siliciclastic-rich intervals were avoided. Carbonate $\delta^{13}C$ and $\delta^{18}O$ isotopic data from the Beck Spring Dolomite were acquired simultaneously at the Scottish Universities Environmental Research Center using an automated triple-collector gas source mass spectrometer (Analytical Precision AP2003), and additional samples of the Virgin Spring Limestone were measured at Harvard University. Approximately 1-mg of micro-drilled samples were reacted in an automated gas-preparation device with H_3PO_4. Evolved CO_2 was collected cryogenically and analyzed using an in-house reference gas. External error (1σ) from standards was better than ± 0.2‰ for both $\delta^{13}C$ and $\delta^{18}O$. Samples were calibrated to VPDB (Vienna Pee-Dee Belemnite) using internal standards and NBS 19. Carbonate $\delta^{13}C$ and $\delta^{18}O$ isotopic results are reported in per mil notation relative to the standard VPDB.

Major and trace element analyses and $^{87}Sr/^{86}Sr$ measurements were performed on 19 samples of the Virgin Spring Limestone collected from the Black Mountains, Saddle Peak Hills, and Southern Ibex Hills (see data repository, Table S2). 50 ± 2 mg of powder was dissolved in Falcon tubes using 5 ml of 1.4M acetic acid. Duplicates were created of a subset of samples and subjected to washing steps with methanol and 0.2M ammonium acetate to remove loosely bound cations from the non-carbonate constituents in the limestone prior to acid dissolution. Tubes were shaken vigorously and placed in an ultrasonic bath for 30 minutes to ensure complete dissolution of the carbonate minerals, and then centrifuged to bead the residue. 3 ml of the affluent was transferred to a clean tube for major and minor element concentrations, and 1 ml to another clean tube for Sr column chemistry.

The concentrations of major and minor elements were measured by solution nebulized-inductively coupled plasma-mass spectrometry (SN-ICP-MS) on a Thermo X series quadrupole at Harvard University. Standard powders BHVO-2, DNC-1, JB-2, and W-2 were used to generate calibration curves. An additional in-house standard K1919 was used to monitor the instrument drift throughout the run. The samples were run with a dilution factor of 1:5K using a matrix solution of 0.2N HNO_3 with Ge (10 ppb), In (3 ppb), Tm (3 ppb) and Bi (3 ppb) as internal standard elements for short-term drift correction. Major and minor elements were measured in two separate but consecutive runs without exchanging any samples, standards, or blanks.

Strontium column chemistry was performed on 1 ml of sample to isolate Sr from coexisting matrix elements. The samples, previously dissolved in acetic acid, were dried and redissolved in 3N nitric acid. This step was repeated three times to ensure that all the acetic acid was evaporated. The solution was then loaded onto a preconditioned Sr Spec column. After three consecutive loadings of 0.25 ml 3N nitric acid to ensure that other elements had been removed, Sr was eluted by 1 reservoir loading (~1ml) of ultrapure water. $^{87}Sr/^{86}Sr$ values were obtained from a Thermo Neptune multicollector ICP-MS at Woods Hole Oceanographic Institute (WHOI), Massachusetts. The measurements were performed with typical ^{88}Sr beam intensities from 30 to 50 volts. $^{87}Sr/^{86}Sr$ ratios were corrected for Kr and Rb, and normalized using the exponential law. The standard NBS 987 was analyzed frequently between samples to monitor the consistency of the measured values.

Micropaleontology

To further refine the biological record bounding Neoproteorzoic glacial events in the context of our new tectonostratigraphic framework, we examined the micropaleontology of the Virgin Spring Limestone, which is the youngest unit preserved directly below the oldest glacial deposits in southeastern Death Valley.

Eighteen samples from the Virgin Spring Limestone from the Black Mountains (with outer weathered surfaces removed) were macerated in acid to obtain residues from which microfossils could be extracted (e.g. Bosak et al., 2011a; Green, 2001) Approximately 10-15 g of coarsely cut sample were washed in a bath of 10% buffered HCl for 24 hours. Clean, prepared samples were then broken into smaller, millimeter-sized pieces and placed in test tubes. Each sample was separately dissolved in 10% HCl and 10% acetic acid to examine yields under different conditions. The residues were then rinsed and filtered over 100 μm, 41 μm, and 0.2 μm Millipore nylon mesh filters using a vacuum filtration device. Organic material was examined in two size fractions, >100 μm and 41-100 μm, under a dissecting microscope and a Nikon ® Eclipse TS100, inverted light microscope. All possible microfossils were picked, mounted on a pin, and coated in mixture of gold and paladium using a Sputter Coater- Hummer V, in preparation for investigation under the FEI Quanta 450 Scanning Electron Microscope (SEM) at the Center for Biological Microscopy and Imaging at Smith College.

RESULTS

Tectonostratigraphic Units

Tectonostratigraphic Unit 0: lower Crystal Spring Formation

We here assign TU0 to the Mesoproterozoic strata of Death Valley to reserve tectonostratigraphic units TU1-TU5 for Neoproterozoic strata, and assign TU1 to early Neoproterozoic strata that are exposed on the northwestern margin of Laurentia but are not present in Death Valley (Macdonald et al., 2012). Correlation of TU0 and TU2 across Death Valley is relatively straightforward, and utilizes the basal unconformity of the lower Crystal Spring Formation and the basal unconformity of the upper Crystal Spring Formation, respectively (Fig. 2). The upper Crystal Spring Formation is not intruded by diabase and rests with an angular discordance of up to 20° on the underlying rocks of the lower Crystal Spring Formation (Mbuyi and Prave, 1993). This unconformity surface defines the base of TU2 and is marked by a sharp contact separating hornfelsed strata below from non-metamorphosed rocks above (Fig. 4a). A decimeter-thick, discontinuous conglomerate and breccia containing abundant hornfels and rare diabase clasts are developed locally along this contact (Fig. 4b). Immediately above these rocks is a widespread sandstone unit that contains detrital zircons as young as ca. 770 Ma (Dehler et al., 2011b). Given the 1.08 Ga date for the diabase, these data suggest that the duration of the lower-upper Crystal Spring Formation unconformity is >300 Ma, spanning deposition of TU1 preserved elsewhere in northern Laurentia (Macdonald et al., 2012).

Tectonostratigraphic Unit 2: upper Crystal Spring Formation, Beck Spring Dolomite and KP1

TU2 consists of the upper Crystal Spring Formation, the Beck Spring Dolomite, and KP1. All three of these units display large lateral facies changes in southeastern Death Valley. Particularly, the Saddle Peak Hills marks an east to west transition from siliciclastic-poor to siliciclastic-rich strata. To the east in the Kingston Range and Alexander Hills, the Beck Springs is a massive, brecciated, dolomitic microbialite (Harwood and Sumner, 2011; Marian and Osborne, 1992) whereas to the west in the Saddle Peak Hills and Southern Ibex Hills it is comprised of hundreds of 1-10 m thick mixed carbonate and siliciclastic parasequences (Fig. 5). In the eastern localities, a variably developed, partially silicified unit of mm- to cm-sized ooids and pebble-sized oncoids occurs near the top of the Beck Spring Dolomite. In the western localities, the Beck Spring Dolomite contains a significant influx of coarse, quartz-rich sediment that is conspicuously absent in the sections east of Saddle Peak Hills. In addition to significant facies changes, the thickness of the Beck Spring Dolomite varies by hundreds of meters (Fig. 5).

The Beck Spring Dolomite passes gradationally (a few to as much as 20 meter-thick transition) into the fine-grained siliciclastic unit KP1 of the Kingston Peak Formation. In many places this interval is marked by interbedded silty carbonate and green-grey siltstone beds and has been referred to as the 'transition beds' (Corsetti and Kaufman, 2003; Link et al., 1993), which are succeeded by up to 250 meters of siliciclastic turbidites of KP1. Historically, KP1 has been placed within the Kingston Peak Formation, but the gradational contact with the underlying Beck Spring Dolomite indicates that it is part of the Beck Spring Dolomite depositional cycle (Prave, 1999). It is noteworthy that no diamictite, dropstones, or any other features that would distinguish KP1 as glaciogenic have ever been documented. When the Pahrump Group stratigraphy is further refined and formalized, we suggest that the upper and lower Crystal Spring Formation are separated into two formations and that unit KP1 is removed from the Kingston Peak Formation (e.g. KP1 was informally referred to as the Saratoga Springs Sandstone by Mrofka, 2010).

Tectonostratigraphic Unit 3: Virgin Spring Limestone, KP2, and KP3

In the Black Mountains, Southern Ibex Hills, and Saddle Peak Hills of southeastern Death Valley (Fig. 1), the Virgin Spring Limestone, a 5-10 m thick unit of black limestone, orange-tan dolostone and minor shale and siltstone, sits unconformably on KP1 (Figs. 6a, 7). It is this unconformity surface that defines the base of Tectonostratigraphic Unit 3. At the type section of the Virgin Spring Limestone in the Black Mountains, the surface is sharp and strata above and below are concordant (Fig. 6b). In the southern Ibex Hills, the contact between the Virgin Spring Limestone and KP1 appears gradational over several tens of centimeters. There, KP1 thins from south to north, from a couple of hundred meters to a few tens of meters, with the loss of section from the top down resulting in an angular discordance with the overlying Virgin Spring Limestone. It is our new mapping in the Saddle Peak Hills, though, that reveals most starkly the unconformable relationship (Fig. 3). There, the Virgin Spring Limestone sits variably on KP1, Beck Spring Dolomite, and the Crystal Spring Formation (Fig. 6a).

The Virgin Spring Limestone displays a complicated internal stratigraphy, varying from limestone- to dolostone-rich and from having abundant to minor siliciclastic interbeds (Fig. 7). Three sections were measured in detail: the eponymous type locality in the Black Mountains, where it is 7 m thick and consists of upper and lower intervals of dark grey, finely laminated carbonate beds separated by an intervening interval of centimeter-thick brown to rust-colored beds containing disseminated silt-sized quartz grains (Fig. 6c); the Southern Ibex Hills where it is 2-3 m thick (Fig. 7), with the basal 0.2 m consisting of interbedded dark grey limestone and siltstone and the remainder being thinly laminated, dark grey calcilutite; and the Saddle Peak Hills, where it is as much as 8 m thick (Fig. 7) and composed predominantly of dark grey limestone interbedded with thin beds of orange to red siltstone and grainstone lenses containing ooids and cobble-sized intraclasts (Fig. 6d). Everywhere, the upper contact with the overlying diamictite of KP2 is erosive (hence the varying thickness from location to location), commonly displaying karst and partial silicification. In many places, the lowermost part of KP2 diamictite contains abundant clasts plucked from the Virgin Spring Limestone, and in the Saddle Peak Hills, there is an 8 m thick interval of orange-weathered dolostone breccia that separates the main body of the Virgin Spring Limestone from the overlying KP2 diamictite.

In the Saddle Peak Hills and Southern Ibex Hills, unit KP2 consists of a massive, dark-weathering diamictite that contains mostly basement clasts. In the Southern Ibex Hills, there are no strata exposed that are stratigraphically above KP2, but in the Saddle Peak Hills a several meter thick arkosic conglomerate-sandstone unit consisting of cm-sized quartz and feldspar grains occurs between massive diamictite of KP2 and stratified diamictite of KP3 (Fig. 8a), testifying to a proximal basement high. This unit has a sharp base and fines upward into KP3. KP3 was subdivided into 3 units for mapping purposes (Fig. 3): KP3a, a thin-bedded to laminated light green-, to buff-, to pink-colored siltstone and sandstone unit with rare dropstones marked by a distinctive black staining along fractures forming an intricately patterned light-dark striping (informally termed 'art rock'); KP3b consisting of matrix- and clast-supported carbonate-clast conglomerate, green- to pale-pink-colored stratified diamictite, thin-bedded fine-grained sandstone and shale with rare drop/lonestones, and very coarse-grained channelized sandstone lenses (Fig. 8b); and KP3c, which is characterized by maroon-colored, thin- to thick-bedded, fine- to very coarse-grained, graded sandstone and siltstone beds with rare lonestones, dropstones, and thin lenses of iron formation, as well as intervals containing dispersed, meter-scale blocks composed predominantly of Beck Spring Dolomite and Crystal Spring Formation. KP3a and KP3b are only present in the southwestern part of the Saddle Peak Hills map area, and both display an overall southwestward thickening. On the southern flank of the Saddle Peak Hills faulting complicates the base of KP3c, but where followed to the southwest towards equivalent beds at Sperry Wash (Abolins et al., 2000; Troxel, 1967), KP3c strata onlap and expand along a low-angle unconformity (Fig. 3).

In the Kingston Range and Alexander Hills, the Virgin Spring Limestone is missing. There, the base of KP2 erodes entirely through the Virgin Spring Limestone to sit directly on KP1. In these instances, the base of KP2 and TU3 are coincident, and the lower part of the KP2 diamictite commonly contains clasts of the Virgin Spring Limestone. In the eastern Kingston Range, massive diamictite of KP2 is overlain by the KP3 megabreccia member of Calzia et al. (1987), which consists of meter to kilometer scale olistoliths in a poorly sorted siliciclastic matrix with striated clasts (Fig. 8c) and contains the "oncolite bed". Previously published maps covering the area of outcrop of the "oncolite bed" show it as a thin, laterally continuous unit sandwiched between the very coarse-grained facies of KP2 and KP3 (Calzia et al. 1987). Our mapping of the "oncolite bed" at several key exposures (including the locality cited by Corsetti et al., 2003) reveals that it is not a continuous unit but actually a series of discontinuous, elongate olisoliths (100s of meters in length), many of which are rotated at a high angle to bedding relative to the encasing Kingston Peak rocks (Figs. 8e, 9). These slabs are associated with other large blocks and slabs that, in effect, form an armada of olistoliths derived largely from the Crystal Spring Formation, the Beck Spring Dolomite, and KP1. In the eastern Kingston Range, the megabreccia member is overlain by >500m of heterolithic gravity flow deposits with minor diamictite and 10-100 m thick bedded iron formation (upper member of Calzia et al., 1987; Graff, 1985). We correlate the megabreccia member to KP3a and KP3b and the upper member to KP3c in the Saddle Peak Hills (Fig. 2).

In the Panamint Mountains, glaciogenic strata of the Limekiln Spring and Surprise members are overlain by a post-glacial succession, the Sourdough cap carbonate and Middle Park Member, which is absent in southeastern Death Valley (Fig. 2). We tentatively place the base of TU3 at the base of the Limekiln Spring Member. We stress that the exact nature of the Limekiln Spring Member remains somewhat enigmatic, in part because of uncertainties in correlations of this unit across the Panamint Range, and will require further work. However, assigning the Limekiln Spring Member to TU3 places the first occurrence of glaciogenic rocks across the Death Valley area into the same succession. This linkage is supported by the presence of arkosic conglomerates in KP3a in the Saddle Peak Hills that share lithological characteristics with the Favorable submember of the Limekiln Spring Member (Carlisle et al., 1980; Kettler, 1982). In the southern and central Panamint Mountains, the Surprise Member consists of massive diamictite intercalated with as much as 60 m of metabasalt (Miller, 1985). To the north these massive diamictite facies grade into a bedded heterolithic sequence. We correlate this sequence, and the Surprise Member in general, to the iron-rich heterolithic beds of KP3c in the Saddle Peak Hills and its equivalent in the eastern Kingston Range (Fig. 2).

Tectonostratigraphic Unit 4: KP4 and the Noonday Formation

In the Saddle Peak Hills, we observed a third diamictite unit, which we attribute to KP4 (Fig. 3). KP4 is distinguished from KP3 by being a coarser and thicker-bedded, massive, matrix-supported diamictite in which the matrix is dark red and consists of silt-sized grains. It infills lenses and channels that erode into KP3 and contains clasts of lithified fragments of the underlying KP3 (Fig. 8d). Further, KP4, along with the capping Noonday Formation, seal NNE-SSW oriented Precambrian faults (e.g. SE corner of Fig. 3). Combined, these observations are evidence for a significant hiatus between KP3 and KP4 and we place the base of TU4 at the base of KP4. Where KP4 is not present, the base of TU4 is coincident with the base of the Noonday Formation.

In the Saddle Peak Hills, we follow Petterson et al.'s (2011) differentiation of the Noonday Formation in the Panamint Mountains into three members: the Sentinel Peak, Radcliff, and Mahogany Flats. On the northern flank of the Saddle Peak Hills, the Sentinel Peak Member is a >100 m thick, light-colored dolomicrite with irregular cements, which locally form giant tubestone stromatolite mounds (Cloud et al., 1974; Corsetti and Grotzinger, 2005; Wright et al., 1978). On the southern flank of the Saddle Peak Hills, the Sentinal Peak member is < 5 m thick and commonly absent where KP4 is overlain by thin-bedded allodapic carbonate and fine to coarse maroon-colored siliciclastic graded beds and debrites of the Radcliffe Member (a.k.a. Ibex facies; Troxel, 1982; Wright and Troxel, 1984). These debrites include tubestone-clast breccias shed off the Sentinal Peak mounds to the north (Fig. 3), and are useful in distinguishing KP4 diamictite and Noonday debrites. The break between massive, thick Sentinal Peak facies and the Ibex facies occurs along the NNW-trending faults that were active during deposition of the underlying strata.

The top of TU4c is placed at the base of the overlying Johnnie Formation, which has been documented as an unconformity (Summa, 1993). In the northern Saddle Peak Hills, karst pipes as much as 10 m deep and filled with coarse quartz grains dissect stromatolitic and laminated dolomicrite of the Mahogany Flats Member. On the southern flanks of those Hills, the lower Johnnie Formation is a many tens of meters thick dolomitic quartz arenite that erodes deeply into the Noonday strata, marking the base of TU5. Unfortunately, in most places the contact is faulted such that it becomes difficult to document the magnitude of the erosional incision.

In the Panamint Range, additional stratigraphy is preserved above the lowermost glaciogenic rocks and the base of TU4 is tentatively placed at the base of the Argenta member, which is a clastic wedge of coarse, arkosic sandstone and conglomerate (Petterson, 2009). An alternative is to place the base of this unit at the base of the Mountain Girl Conglomerate. Which of these two surfaces is the more correct remains to be substantiated, but in either case, both surfaces seal an episode of deformation: the base of the clastic wedge of the Argenta member sits locally with angular discordance on underlying rocks whereas the Mountain Girl Conglomerate appears to cut across the Argenta wedge (Petterson, 2009).

The subdivision of TU4 into TU4a, TU4b, and TU4c, highlights the syntectonic deposition and wedge-shaped stratal geometries (Fig. 2). TU4a consists of granitic grit and fanglomerate of the Argenta member (Petterson, 2009). The Argenta fanglomerate is sharply overlain by the conglomeratic Mountain Girl Member, which in turn is sharply overlain by the Thorndike Limestone; these units constitute TU4b. TU4a and TU4b are absent in southeastern Death Valley. The base of the overlying massive diamictite of the Wildrose Diamictite, which commonly has an erosive base and cuts variably through the underlying strata (e.g. Prave, 1999), defines the base of TU4c. The Sentinel Peak Member of the Noonday Formation caps the Wildrose Diamictite, which is equivalent to KP4 in southeastern Death Valley (e.g. Prave, 1999). Where the diamictite is missing, the base of TU4c becomes coincident with the base of the Sentinel Peak Member.

Chemostratigraphy

Beck Spring Dolomite

The base of the Beck Spring Dolomite exhibits negative C-isotopic values, reaching a nadir of -3‰. Values increase up-section to a plateau of ~+5‰, with persistent positive values through the bulk of the formation before a downturn to -3 to -5‰ at the top (Fig. 5). This trend is consistent with the findings of previous workers (Prave, 1999; Corsetti and Kaufman, 2003). The upper negative excursion is best developed in the Kingston Range (Fig. 5) and, relevant for the discussion to follow, is present within a distinctive oncolite-bearing dolostone bed.

Virgin Spring Limestone

The $\delta^{13}C$ data from the Virgin Spring Limestone range from +1 to +7‰ (Fig. 7), and show variable profiles from section to section. The values nevertheless distinguish the Virgin Spring Limestone from the isotopically depleted Sourdough Limestone (Prave, 1999; Corsetti & Kaufman, 2003; Peterson et al., 2011), but are similar to those of the ^{13}C-enriched Thorndike Limestone.

Several Virgin Spring Limestone samples contain low Rb concentrations and very high Sr concentrations at an average of ~2300 ppm for unwashed samples (see data repository). The latter suggests that the Virgin Spring Limestone was originally precipitated as aragonite, which is supported by petrographic analyses of Tucker (1986). However, most of the $^{87}Sr/^{86}Sr$ values in both washed and unwashed samples is highly radiogenic, indicating contamination either from fine disseminated clay or from fluids enriched in radiogenic Sr and/or Rb. Further, the data show a weak relationship between Sr concentration and $^{87}Sr/^{86}Sr$ values, and Sr isotope values co-vary with both the abundance of Rb and with Mn/Sr ratios (see data repository, Table S2). These results indicate that the Virgin Spring Limestone has suffered from significant diagenesis. Consequently, because diagenetic fluid flow from crustally derived sources generally increases the Sr isotopic ratio to more radiogenic values, we surmise that the lowest $^{87}Sr/^{86}Sr$ ratios would represent the best estimates for primary $^{87}Sr/^{86}Sr$ composition.

Most Virgin Spring Limestone samples from the type locality yielded high $^{87}Sr/^{86}Sr$ values, near 0.71 (see data repository, Table S2). Samples from the Saddle Peak and Southern Ibex Hills sections were generally less radiogenic. The lowest value of 0.70676 came from a limestone sampled near the base of the Saddle Peak Hills section. This sample was measured several times, and the result was reproduced consistently.

Thus, we consider 0.70676 as the best estimate for the least-altered $^{87}Sr/^{86}Sr$ value of the Virgin Spring Limestone.

"Oncolite Bed" in KP3

Carbon isotope values in the "oncolite bed" in KP3 increase upwards from -2.5‰ to -0.5‰ (Fig. 10, data repository, Table S1), excluding one negative outlier.

Micropaleontology

Microfossils were observed both *in situ* in thin sections and in residues of the Virgin Spring Limestone. The microfossils extracted were sparse but several common morphotypes were documented from 6 samples (see Fig. 7 for stratigraphic position) and these can be separated into two distinct groups based on morphological characteristics: some possible VSMs and organic material that lacked a robust test (Fig. 11). The former exhibit oval or spheroidal shapes extending into a neck or tapering to a point, and share features reported previously for VSMs (Marti-Mus and Moczydlowska, 2000; Porter and Knoll, 2000) (Figs. 11a, 11c, 11e). They have lengths between 100–200 µm and widths between 100–120 µm (mean length of ~120 µm; N=6 whole tests and N=18 broken tests), and a few have putative apertures (Figs. 11a, 11c, 11e). Some have characteristics of modern lobose testate amoebae Hyalospheniidae, within Tubulinea (Fig. 11a), such as a smooth test similar to *Nebela sp.* (Fig. 11b). Others exhibit a cratered texture, and the surface indentations have a diameter of 10µm with a 2µm rim (Fig. 11c) that is similar to modern test, *Nebela penardiana* (Fig. 11d), which secretes siliceous scales. In addition, size are comparable to modern populations (Ogden and Hedley, 1980). Although these ancient forms exhibit broad similarities to modern testate amoebae, we cannot assign them with confidence to modern groups.

Organic forms that lack a robust mineralized test were also observed in filtered residue samples of the Virgin Spring Limestone from the Black Mountains (N=7). Many resemble filaments, tubes, and/or possible remnants of cyanobacteria or algae (Fig. 11f, 11g). Filaments range in size from 800μm to several mm in length and in thickness from 10–20μm, and some appear to be hollow or attached to a possible collapsed vesicle (Fig. 11f). Some forms exhibited a flat, wide, elongate morphology (Fig. 11g) and resemble previously identified forms, such as the cyanobacterial sheath, *Siphonophycus solidum* (Vorob'eva et al., 2009).

DISCUSSION

Our new mapping, stratigraphic observations, and geochemistry allow us to refine regional correlations and integrate these records globally. Below we discuss how regional chemostratigraphic correlations help us refine our tectonostratigraphic units and the stratigraphic position of the fossiliferous "oncolite bed". We then extend these correlations to key successions along the western margin of Laurentia with paleontological data and geochronological control to construct an age model and discuss the implications for the relationship between the Neoproterozoic microfossil and glacial records, the nature of Neoproterozoic iron formations, and the tectonic evolution of the supercontinent Rodinia.

Carbon and Strontium Isotope Chemostratigraphy

Previous workers have used the apparent covariance in the $\delta^{13}C$ and $\delta^{18}O$ composition of carbonate rocks in Death Valley to argue that these values have been severely modified by meteoric alteration (e.g. Kenny and Knauth, 2001; Knauth and Kennedy, 2009). The new $\delta^{13}C$ and $\delta^{18}O$ data that we present do not covary (see data repository Tables S1 and S2) and a qualitative covariance can be observed for carbonate carbon and organic carbon isotopes through the negative anomaly at the top of the Beck Spring Dolomite (Corsetti & Kaufman, 2003), which we correlate with the Islay anomaly (Hoffman et al., 2012). Although there is certainly some alteration of the original isotopic signals, we conclude that the majority of our $\delta^{13}C$ values reflect the primary dissolved inorganic carbon isotope composition of the basin. The exception is the negative carbonate carbon isotope values associated with karsted intervals near the top of the Virgin Spring Limestone. These values covary with oxygen isotopes and likely reflect modification of an original primary signal. Using our new data, along with previous data (Corsetti and Kaufman, 2003; Petterson et al., 2011; Prave, 1999), we constructed a composite carbonate carbon isotope curve recast in the framework of our new correlation scheme (Fig. 12).

The Virgin Spring Limestone has been previously correlated with the Sourdough Limestone (Tucker, 1986) and the Thorndike Limestone. Isotopically enriched $\delta^{13}C$ values distinguish the Virgin Spring Limestone from the depleted $\delta^{13}C$ values of the Sourdough Limestone (Prave, 1999; Corsetti & Kaufman, 2003; Peterson et al., 2011), but are similar those of the Thorndike Limestone. To test the plausibility of correlating the Virgin Spring Limestone to the Thorndike, we can utilize our new $^{87}Sr/^{86}Sr$ data on the Virgin Spring Limestone. The metamorphic grade in the Panamint Mountains precludes obtaining reliable primary $^{87}Sr/^{86}Sr$ ratios in the Thorndike Limestone. But, the

Thorndike Limestone is part of the inter-glacial succession whereas in our proposed framework, the Virgin Spring Limestone pre-dates the glaciations (Fig. 2). Thus, correlations could be tested by comparing the $^{87}Sr/^{86}Sr$ values in the Virgin Spring Limestone to the composite strontium isotope curves for the Cryogenian (Halverson et al., 2007; Halverson et al., 2010). A composite Cryogenian strontium isotope curve was constructed (Fig. 12, data repository Table S3) by modifying that of Halverson et al. (2007; 2010) by adding additional data from Mongolia (Brasier et al., 1996; Shields et al., 2002), Scotland (Sawaki et al., 2010), Greenland (Fairchild et al., 2000), and NW Canada (Halverson et al., 2007). This composite shows that pre-Sturtian $^{87}Sr/^{86}Sr$ values are below ~0.707, and aside from the Sturtian cap carbonate, $^{87}Sr/^{86}Sr$ values between the Sturtian and Marinoan are above ~0.707 (Fig. 12).

Virgin Spring Limestone samples from the type locality yielded extremely radiogenic $^{87}Sr/^{86}Sr$ values (>0.71) that were much higher than samples from the Saddle Peak and Southern Ibex Hills sections (see data repository). We suggest this regional difference is due to enhanced local fluid flow related to Neogene extension and plutonism along the Black Mountains detachment (Calzia and Ramo, 2000; Wright and Troxel, 1984). This scenario is consistent with petrographic and field observations of intense veining along tension gashes (Fig. 6b) throughout the exposures in the Black Mountains.

The lowest $^{87}Sr/^{86}Sr$ values of the Virgin Spring Limestone were from samples collected on the southern side of the Saddle Peak Hills (Fig. 3). These exposures are >30 km away from the nearest break-away detachment (Calzia and Ramo, 2000), and consequently may not have been as intensely flushed with basement-derived fluids as the samples from the Black Mountains. Values as low as ~0.70676 are consistent with

$^{87}Sr/^{86}Sr$ values of pre-Sturtian strata or Sturtian cap carbonates (Fig. 12). However, unlike Sturtian cap carbonates, such as the Sourdough Limestone, the Virgin Spring Limestone sits below, not above glacial deposits, and it has enriched instead of depleted $\delta^{13}C$ values. Thus, we suggest the Virgin Spring Limestone is pre-Sturtian in age and is neither correlative with the post-Sturtian Sourdough Limestone nor the pre-Marinoan Thorndike Limestone. The enriched $\delta^{13}C$ values are further similar to Bed Group 20 in Greenland, which sits above the Isaly anomaly but below Sturtian glacial deposits (Fairchild et al., 2000).

Stratigraphic Position of the "Oncolite Bed"

The "oncolite bed" has previously been cited as the only known example of a syn-glacial microfossil assemblage, and has been used to question the severity of Snowball Earth conditions (Corsetti, 2009; Corsetti et al., 2003; Corsetti et al., 2006). Our mapping demonstrates that the fossiliferous oncolite-bearing dolostone layer in the eastern Kingston Range is a series of olistoliths (Fig. 9). We correlate these olistoliths with a lithologically indistinguishable oncolite-bearing interval in the uppermost Beck Spring Dolomite (Fig. 13). To further test this correlation, we compared $\delta^{13}C$ values between measured stratigraphic sections of the oncolite olistoliths in the eastern Kingston Range with oncolite-bearing beds of the uppermost Beck Spring Dolomite. Carbon isotope profiles through both contain a negative $\delta^{13}C$ values, consistent with our correlation. Thus, we conclude that fossils previously reported as representative of syn-glacial ecosystems (Corsetti, 2009; Corsetti et al., 2003; Corsetti et al., 2006) are in fact representative of the pre-glacial, <770 Ma and >717 Ma uppermost Beck Spring Dolomite.

Previous workers have mistakenly mapped the oncolite blocks as an *in situ* bed because the blocks have large aspect ratios (length:thickness) and tend to be aligned roughly with the bedding of KP3. This geometric orientation is to be expected in that the original organization of the oncolitic interval at the top of the Beck Spring Formation, from which the blocks where derived, consists of meters-thick oncolite layers interbedded with recessive shaley intervals. Hence, we envisage the emplacement of the oncolitic olistoliths as tabular-shaped slide blocks dislodged from the weaker shaley intervals whereas the more massive Beck Spring Dolomite olistoliths were emplaced as more chaotically redeposited blocks. The probable break away-scarp (likely having considerable relief) would have been located ~ 2 km to the northeast, between the *in situ* Beck Springs outcrop belt forming a high ridge along the northern flank of the Kingston Range and the olistolith-rich KP3 unit in the mapped area of the eastern Kingston Range.

Laurentian Correlations

Geochronological constraints on Neoproterozoic strata in the Grand Canyon, Idaho, and northwestern Canada make it attractive to correlate between the Pahrump Group and other Neoproterozoic successions along Laurentia's margin (Fig. 14). Microfossil assemblages and chemostratigraphy permit correlating TU2 broadly to the 770–740 Ma Chuar Group in the Grand Canyon (Karlstrom et al., 2000; Porter et al., 2003) and Uinta Mountains Group in Utah (Dehler et al., 2010). Hoffman et al. (2012) suggested that the negative $\delta^{13}C$ anomaly at the top of the Beck Spring Dolomite is regionally correlative with the negative $\delta^{13}C$ anomaly in the lower portion of the Coppercap Formation in NW Canada (Halverson, 2006), and that both are globally correlative to the pre-Sturtian Islay anomaly. Thus, we suggest that the upper Crystal Spring Formation and much of the Beck Spring Dolomite is correlative with the Chuar Group and was deposited between ~770 and 740 Ma (Fig. 14). The uppermost Beck Spring Dolomite and KP1 may be correlative with the lower Coppercap Formation. Strontium and carbon isotope chemostratigraphy further support a correlation between the Virgin Spring Limestone and the pre-717 Ma uppermost Coppercap Formation (Fig. 12), which records a return to positive $\delta^{13}C$ values (Halverson, 2006; Halverson et al., 2007).

An array of ages bracket the Sturtian glaciation(s) to within a ca. 50 Myr window: the 717.4 ± 0.2 Ma and 716.5 ± 0.2 Ma U-Pb zircon dates from the Mount Harper Volcanic Complex (Macdonald et al., 2010a); the ca. 663 Ma U-Pb ages on the Datangpo Formation in South China (Zhou et al., 2004), and the Wilyerpa Formation in Australia (Fanning & Link, 2008); and the syn-Sturtian U-Pb zircon age constraints of 687.4 ± 1.3 Ma and 685.5 ± 0.4 from Idaho (Condon and Bowring, 2011; Keeley et al., 2013) and 711.5 ± 0.3 from Oman (Bowring et al., 2007). Other previously reported age constraints on glaciogenic strata in Idaho (Fanning and Link, 2004) have been shown to be inherited or detrital (Dehler et al., 2011a; Keeley et al., 2013), whereas the stratigraphic context of ages from high-grade sequences in central Idaho is uncertain (Lund et al., 2010; Lund et al., 2003). Given our new Death Valley data, the KP2–KP3–Limekiln Spring–Surprise diamictites can be correlated with the 717-663 Ma Rapitan Group (Macdonald et al., 2010a), making the Sourdough Limestone correlative with the ca. 662 Ma Twitya cap carbonate, the Thorndike Limestone with the Keele Formation and enriched $\delta^{13}C$ values of the ‘Keele Peak’ (Kaufman et al., 1997), and the KP4–Wildrose diamictites with the Marinoan glacial deposits of the Ice Brook Formation (Aitken, 1991a; Aitken, 1991b; Hoffman and Halverson, 2011). As shown previously (Prave, 199; Petterson et al., 2011), the Sentinel Peak Member of the Noonday Formation can be correlated to ca. 635 Ma Ediacaran cap carbonates worldwide (Condon et al., 2005), including the Ravensthroat Formation (James et al., 2001).

Micropaleontology

The pre-717 Ma microfossil record contains evidence for the diversification of six eukaryotic crown groups: amoebozoa, rhizaria, stramenopiles, fungi, red algae, and green algae (see references in Knoll et al., 2006; Macdonald et al., 2010b); although some of these fossils could be represent stem groups (e.g. Berney and Pawlowski, 2006). On the western margin of Laurentia (Fig. 14), this record includes VSMs in the ca. 770-742 Ma Chuar Group in the Grand Canyon (Porter et al., 2003), scale microfossils of possible green algal affinity from northwestern Canada (Allison, 1980; Allison and Hilgert, 1986; Cohen and Knoll, 2012; Cohen et al., 2011; Macdonald et al., 2010a), and VSMs, filamentous organisms, possible algae, and cyanobacteria from the Pahrump Group (Corsetti et al., 2003; Licari, 1978; Pierce and Cloud, 1979). The latter occurrences were from the Beck Spring Dolomite, KP1, and the “oncolite bed” sampled from the Alexander Hills and the Kingston Range. The reassignment of the “oncolite bed” to the Beck Spring Dolomite and the identification of possible VSMs in the Virgin Spring Limestone, suggests that the Virgin Spring VSMs represent the youngest described to date in the Cordillera (Fig. 14). Moreover, all of these microfossil assemblages in the

Pahrump Group are pre-Sturtian in age. To assess the biological response to the Sturtian glaciation in Death Valley, the microfossil record of the post-Sturtian Sourdough Formation would need to be examined; however, the high metamorphic-grade of exposures in the Panamint Mountains may have left these strata inappropriate for micropaleontological investigations. More broadly, VSMs appear to be common globally in pre-Sturtian successions, whereas a variety of tests and agglutinating microfossils are present in assemblages deposited during the Cryogenian non-glacial interlude (Bosak et al., 2011a; Bosak et al., 2012; Bosak et al., 2011b; Pruss et al., 2010). The degree to which this apparent change is a function of taphonomy or biological turnover remains to be determined.

Sturtian-Rapitan Iron Formations

Mrofka and Kennedy (2011) suggest that iron formation in the Kingston Peak Formation is the product of Neogene volcanism. However, locally there is no strong relationship between the distribution of iron formation and Neogene volcanism. Instead, the correlation of KP3 with the Surprise Member suggests contemporaneity between deposition of iron formation in KP3 (Abolins et al., 2000; Calzia et al., 1987; Graff, 1985) and basalt eruptions in the Surprise Member (Miller, 1985). This correlation is further supported by the identification of volcaniclastic material in the upper member of KP3 in the eastern Kingston Range (Calzia et al., 1987; Graff, 1985). These results are consistent with the conclusion of Macdonald et al. (2010c) that the vast majority of Neoproterozoic iron formations are of Sturtian age. The combination of lowered sea-level during glaciation, restriction in narrow, actively rifting basins, favorable Fe/S ratios in the ocean, and enhanced hydrothermal activity in proximity to volcanic rocks, including large igneous provinces, may have conspired as a perfect backdrop for iron formation and their return to the rock record after a billion year absence (Bekker et al., 2010). It is also worth noting the similarities between KP3c and the Sayunei Formation in northwestern Canada. Both are composed of maroon-colored turbidites and debris flows with sporadic dropstones, and both formed during active extension and adjacent to active volcanism (Macdonald et al., 2010a).

Tectonic Evolution

Neoproterozoic conglomeratic and volcanic rocks exposed within the North American Cordillera have long been interpreted as synrift deposits (Stewart, 1975), representing the breakup of the supercontinent Rodinia (Dalziel, 1991; Hoffman, 1991; Moores, 1991). However, the number of rifting events, the timing and geometry of breakup, the arrangement of cratons, and the relationship to large igneous provinces (LIPs) have remained poorly constrained (e.g. Dalziel, 1997; Evans, 2009; Goodge et al., 2008; Li et al., 2008; Sears, 2012; Sears and Price, 2003). Geological arguments have been made for multiple or protracted rifting episodes on the western margin of Laurentia at 780–740 Ma (Jefferson and Parrish, 1989; Karlstrom et al., 2000), 720–635 Ma (Eisbacher, 1985; Lund et al., 2003; Prave, 1999), and 580–560 Ma (Colpron et al., 2002). Although the latter is consistent with subsidence analyses that indicate a rift-drift transition near the Precambrian-Cambrian boundary at ca. 540 Ma (Armin and Mayer, 1983; Bond and Kominz, 1984), this leaves >200 Myrs of enigmatic basin development.

The identification of major unconformities, their regional correlation, and the construction of an age model, creates a new framework for the Neoproterozoic tectonic evolution of the southwestern margin of Laurentia (Fig. 14). The bases of TU2 and TU3 represent major basin-forming events, accommodating kilometer-scale subsidence with distinct and different patterns. The lower Crystal Spring-upper Crystal Spring unconformity records large-scale regional tilting and a major hiatus. The unconformity is succeeded by well-developed parasequences of the upper Crystal Spring Formation and Beck Spring Dolomite. We suggest that large lateral facies changes and thickness variations in the Beck Spring Dolomite are the result of syndepositional faulting. The Beck Spring-KP1 transition represents a major drowning and influx of fine siliciclastic material to the basin. Subsequently, additional faults, folds, and high-angle unconformities developed, all of which are sealed by the Virgin Spring Limestone (Fig. 3) or the stratigraphically lowest diamictite at several localities (Labotka et al., 1980; MacLean et al., 2009; Miller, 1985; Walker et al., 1986). TU2 of Death Valley, that is the upper Crystal Spring Formation and the Beck Spring Dolomite, are potentially correlative with the Chuar Group of the Grand Canyon and Uinta Mountains Group of Utah, which also host a major deepening prior to a pre-Sturtian unconformity (Dehler et al., 2010). It has been suggested that these successions formed during an early phase of Rodinian extension, and that the Chuar Group in particular was accommodated by syn-depositional faulting along the Butte fault (Timmons et al., 2001). In northwestern Canada, this basin-forming episode can also be correlated with that which accommodated the Callison Lake and Coates Lake groups (Fig. 14; Macdonald et al., 2010a; Jefferson & Parrish, 1992).

In northwestern Canada, syn-sedimentary faulting persisted throughout deposition of the Rapitan Group and the ca. 650 Ma Keele Formation (Eisbacher, 1981). Our age model would suggest that Cryogenian tectonism also persisted in southwestern Laurentia (present coordinates) through the Sturtian glaciation, consistent with recent paleomagnetic reconstructions (Li and Evans, 2011). Olistoliths are common in KP3, and coincide with an expansion in KP3 on the southwestern side of the Saddle Peak Hills (Fig. 3). The likely correlative strata in the Panamint Mountains grade from finer-grained and probably deeper-water deposits southward into massive diamictite of the Surprise Member (Miller, 1985). Restoration of Mesozoic thrusting and Neogene extension and translation places the northern Panamint Mountains at a position closer to the Saddle Peak Hills (see Figure 13 of Petterson et al., 2011). In this restoration, stratified diamictite and coarse-grained sediment-gravity-flow deposits of KP3 are present in a NW-SE oriented band, which potentially formed in a narrow graben.

In the Saddle Peak Hills, Precambrian faults and associated angular unconformities are capped by the sub-KP4 erosional unconformity. Thus, in the Saddle Peak Hills we cannot distinguish TU3 and TU4 structures. TU3 is manifested in granitic grits, fanglomerates, olistostromes and unconformities, and we infer that faulting during TU4 time reactivated TU3 structures, resulting in dramatic paleo-topography and lateral facies changes in the basal Noonday Formation. Thus, we suggest that Cryogenian tectonism in Death Valley records the formation of narrow grabens during multiple modest extensional events with low stretching factors. It is possible that true rifting of the western margin of Laurentia did not occur until the latest Ediacaran, which is represented by TU5 (Fig. 14), and was followed by broad regional subsidence in the early Paleozoic (Armin and Mayer, 1983).

It has been suggested that the Neoproterozoic-Mesozoic deposits of Death Valley formed on a ribbon continent Rubia that was separated from North America until the Cretaceous Cordilleran orogeny (Hildebrand, 2009). The strong similarities between Neoproterozoic tectonostratigraphic packages in Death Valley and truly autochthonous successions in the Grand Canyon and northwestern Canada (Fig. 14) tightens the noose around Rubia, and suggests, if it did ever exist, it must have separated from Laurentia during the Ediacaran.

Conclusion

Mapping of the Proterozoic Pahrump Group in the Saddle Peak Hills and the Kingston Range has facilitated correlations between the Panamint Mountains and southeastern Death Valley. We have identified four temporally and spatially distinct tectono-stratigraphic packages within the Pahrump Group. Combined with new C and Sr isotopic data, these data suggest that units KP2 and KP3 of the Kingston Peak Formation are regionally correlative with the Limekiln Spring and Surprise members in the Panamint Mountains and globally correlative with the Sturtian glaciation. Our integrated geological mapping and isotope chemostratigraphy has also demonstrated that a microfossil-bearing "oncolite bed" in KP3 is an olistostrome sourced from the top of the Beck Spring Dolomite (Fig. 13). Four unconformity-bound tectonostratigraphic successions have been identified in the Neoproterozoic succession of Death Valley. The oldest defines the base of the upper Crystal Spring Formation (and records a ca. 300 Myr duration unconformity), two are intra-Kingston Peak Formation, and the last is at the base of the Johnnie Formation. These surfaces are used to construct correlations to sections elsewhere across western Laurentia that have better geochronological control and indicate that the upper Crystal Spring through Noonday formations in Death Valley were deposited between ca. 770 and 635 Ma, a time window containing both of the main Cryogenian glaciations and an episode of extensional tectonism. We further report the presence of a younger microfossil assemblage in the Virgin Spring Limestone, which underlies units KP2 and KP3. All microfossil assemblages discovered to date from the Pahrump Group are pre-Sturtian in age and can no longer be used to independently assess the severity of the glaciations represented in the Kingston Peak Formation (c.f. Corsetti, 2009; Corsetti et al., 2003; Corsetti et al., 2006). Although it is clear that eukaryotes survived and flourished in the aftermath of the Sturtian Snowball (Bosak et al., 2011a), the current biological record is too coarse to determine if the glaciations were the cause of extinctions or radiations of eukaryotic organisms.

ACKNOWLEDGEMENTS

We thank the NAI MIT node for support. We thank the 2012 and 2013 Harvard University EPS 74 Field Geology class for contributions to the mapping. We thank P. Hedman, W. Macdonald for their cooking. We thank Harvard's EPS Department for providing logistics for EPS 74, field trips to Death Valley, and support for R. Petterson's post-doctoral work. We thank MIT EAPS for use of their field supplies. We thank D. Schrag, C. Langmuir, Z. Chen, and G. Eischeid for use and assistance of laboratories at Harvard University. We thank E. Sperling, S. Petersen, L. Dalton, S. Westacott, and J.

Loveless for help in the field, M. Vollinger for thin section assistance, and Smith College for partial funding of this work. We thank the National Park Service at Death Valley for permitting us to sample within the Park. We thank R. Mahon, C. Dehler, F. Corsetti, E. Sperling and an anonymous reviewer for helpful comments on the manuscript.

REFERENCES

Abolins, M., Oskin, R., Prave, T., Summa, C., and Corsetti, F. A., 2000, Neoproterozoic glacial record in the Death Valley region, California and Nevada, *in* Lageson, D. R., Peters, S. G., and Lahren, M. M., eds., Great Basin and Sierra Nevada, Volume Field Guide 2: Boulder, CO, Geological Society of America, p. 319-335.

Aitken, J. D., 1991a, The Ice Brook Formation and Post-Rapitan, Late Proterozoic glaciation, Mackenzie Mountains, Northwest Territories: Geological Survey of Canada Bulletin, v. 404, p. 1-43.

Aitken, J. D., 1991b, Two late Proterozoic glaciations, Mackenzie Mountains, northwestern Canada: Geology, v. 19, no. 5, p. 445-448.

Allison, C. W. A., 1980, Siliceous microfossils from the lower Cambrian of northwest Canada: Possible source for biogenic chert: Science, v. 211, p. 53-55.

Allison, C. W. A., and Hilgert, J. W., 1986, Scale micro-fossils from the Early Cambrian of northwest Canada: Journal of Paleontology, v. 60, p. 973-1015.

Armin, R. A., and Mayer, L., 1983, Subsidence analysis of the Cordilleran miogeocline: Implications for timing of Late Proterozoic rifting and amount of extension: Geology, v. 11, p. 702-705.

Barth, A. P., Wooden, J. L., Coleman, D. S., and Fanning, C. M., 2000, Geochronology of the Proterozoic basement of southwesternmost North America and the origin and evolution of the Mojave crustal province: Tectonics, v. 19, p. 616-629.

Bekker, A., Slack, J. F., Planavsky, N., Krapez, B., Hofmann, A., Konhauser, K. O., and Rouxel, O. J., 2010, Iron formation: The sedimentary product of a complex interplay among mantle, tectonic, oceanic, and biospheric processes: Economic Geology, v. 105, p. 467-508.

Berney, C., and Pawlowski, J., 2006, A molecular time-scale for eukaryote evolution recalibrated with the continuous microfossil record: Proceedings of the Royal Society B: Biological Sciences, v. 273, no. 1596, p. 1867-1872.

Bond, G. C., and Kominz, M. A., 1984, Construction of tectonic subsidence curves for the early Paleozoic miogeocline, southern Canadian Rocky Mountains: implications for subsidence mechanisms, age of breakup, and crustal thinning: Geological Society of America Bulletin, v. 95, no. 2, p. 155-173.

Bosak, T., Lahr, D. J. G., Pruss, S. B., Macdonald, F. A., Dalton, L., and Matys, E., 2011a, Agglutinated tests in post-Sturtian cap carbonates of Namibia and Mongolia: Earth and Planetary Science Letters, v. 308, p. 29-40.

Bosak, T., Lahr, D. J. G., Pruss, S. B., Macdonald, F. A., Gooday, A. J., Dalton, L., and Matys, E., 2012, Possible early foraminiferans in post-Sturtian (716-635 Ma) cap carbonates: Geology, v. 40, no. 1, p. 67-70.

Bosak, T., Macdonald, F. A., Lahr, D. J. G., and Matys, E., 2011b, Putative Cryogenian ciliates from Mongolia: Geology, v. 39, no. 12, p. 1123-1126.

Bowring, S. A., Grotzinger, J. P., Condon, D. J., Ramezani, J., and Newall, M., 2007, Geochronologic constraints on the chronostratigraphic framework of the Neoproterozoic Huqf Supergroup, Sultanate of Oman: American Journal of Science, v. 307, p. 1097-1145.

Boyle, R. A., Lenton, T. M., and Williams, H. T. P., 2007, Neoproterozoic 'snowball Earth' glaciations and the evolution of altruism: Geobiology, v. 5, no. 4, p. 337-349.

Brain, C. K., Prave, A. R., Hoffmann, K. H., Fallick, A. E., Botha, A., Herd, D. A., Sturrock, C., Young, I., Condon, D. J., and Allison, S. G., 2012, The first animals: ca. 760-million-year-old sponge-like fossils from Namibia: South African Journal of Science, v. 108, no. 1/2 #658, p. 1-8.

Brasier, M. D., Shields, G., Kuleshov, V. N., and Zhegallo, E. A., 1996, Integrated chemo- and biostratigraphic calibration of early animal evolution: Neoproterozoic -early Cambrian of southwest Mongolia: Geological Magazine, v. 133, no. 4, p. 445-485.

Burchfiel, B. C., Cowan, D. S., and Davis, G. A., 1992, Tectonic overview of the Cordilleran orogen in the western United States, *in* Burchfiel, B. C., Lipman, P. W., and Zoback, M. L., eds., The Geology of North America, Volume G-3, The Cordilleran Orogen: Conterminous U.S.: Boulder, Geological Society of America, p. 407-479.

Burchfiel, B. C., Pelton, P. J., and Sutter, J., 1970, An early Mesozoic deformation belt in south-central Nevada-southeasterrn California: Geological Society of America Bulletin, v. 81, p. 211-215.

Calzia, J. P., 1990, Geologic studies in the Kingston Range, southern Death Valley, California [Ph. D: University of California, 159 p.

Calzia, J. P., Frisken, J. G., Jachens, R. C., McMahon, A. B., and Runsey, C. M., 1987, Mineral resources of the Kingston Ranges Wilderness Study Area, San Bernardino County, California: U.S. Geological Survey Bulletin, v. 1709-C, p. 1-21.

Calzia, J. P., and Ramo, O. T., 2000, Late Cenozoic crustal extension and magmatism, southern Death Valley region, California, *in* Lageson, D. R., Peters, S. G., and Lahren, M. M., eds., Great Basin and Sierra Nevada, Volume Field Guide 2: Boulder, CO, Geological Society of America, p. 135-164.

Carlisle, D., Kettler, R. M., and Swanson, S. C., 1980, Geological study of uranium potential of the Kingston Peak Formation, Death Valley region, Californian, Grand Junction, CO, U.S. Department of Energy Open-File Report.

Cloud, P. E., Jr., Wright, L. A., Williams, E. G., Diehl, P., and Walter, M. R., 1974, Giant stromatolites and associated vertical tubes from the Upper Proterozoic Noonday Dolomite, Death Valley region, eastern California: Geological Society of America Bulletin, v. 85, p. 1869-1882.

Cohen, P. A., and Knoll, A. H., 2012, Scale microfossils from the mid-Neoproterozoic Fifteenmile Group, Yukon Territory: Journal of Paleontology, v. 86, no. 5, p. 775-800.

Cohen, P. A., Schopf, J. W., Kudryaytsev, A., Butterfield, N. J., and Macdonald, F. A., 2011, Phosphate biomineralization in mid-Neoproterozoic protists: Geology, v. 39, no. 6, p. 539-542.

Colpron, M., Logan, J. M., and Mortensen, J. K., 2002, U-Pb zircon age constraint for late Neoproterozoic rifting and initiation of the lower Paleozoic passive margin of western Laurentia: Canadian Journal of Earth Sciences, v. 39, p. 133-143.

Condon, D. J., and Bowring, S. A., 2011, A user's guide to Neoproterozoic geochronology, *in* Arnaud, E., Halverson, G. P., and Shields-Zhou, G., eds., The Geological Record of Neoproterozoic Glaciations, Volume 36: London, Geological Society, p. 135-149.

Condon, D. J., Zhu, M., Bowring, S. A., Wang, W., Yang, A., and Jin, Y., 2005, U-Pb ages from the Neoproterozoic Doushantuo Formation, China: Science, v. 308, p. 95-98.

Corsetti, F. A., 2009, Extinction before the snowball: Nature Geoscience, v. 2, p. 386-387.

Corsetti, F. A., Awramik, S. M., and Pierce, D., 2003, A complex microbiota from snowball Earth times: Microfossils from the Neoproterozoic Kingston Peak Formation, Death Valley, USA: Proceedings of the National Academy of Sciences, v. 100, no. 8, p. 4399-4404.

Corsetti, F. A., and Grotzinger, J. P., 2005, Origin and significance of tube structures in Neoproterozoic post-glacial cap carbonates: example from Noonday Dolomite, Death Valley, United States: Palaios, v. 20, p. 348-363.

Corsetti, F. A., and Hagadorn, J. W., 2000, Precambrian-Cambrian transition: Death Valley, United States: Geology, v. 28, no. 4, p. 299-302.

Corsetti, F. A., and Kaufman, A. J., 2003, Stratigraphic investigations of carbon isotope anomalies and Neoproterozoic ice ages in Death Valley, California: Geological Society of America Bulletin, v. 115, no. 8, p. 916-932.

Corsetti, F. A., Olcott, A. N., and Bakermans, C., 2006, The biotic response to Neoproterozoic snowball Earth: Palaeogeography Palaeoclimatology Palaeoecology, v. 232, no. 2-4, p. 114-130.

Costas, E., Flores-Moya, A., and Lopez-Rodas, V., 2008, Rapid adaptation of phytoplankters to geothermal waters is achieved by single mutations: Were extreme environments 'Noah's Arks' for photosynthesizers during the Neoproterozoic 'Snowball Earth'?: New Phytologist, v. 180, no. 4, p. 922-932.

Dalziel, I. W. D., 1991, Pacific margins of Laurentia and East Antarctica-Australia as a conjugate rift pair: Evidence and implications for an Eocambrian supercontinent: Geology, v. 19, p. 598-601.

-, 1997, Neoproterozoic-Paleozoic geography and tectonics: review, hypothesis, environmental speculation: Geological Society of America Bulletin, v. 109, p. 16-42.

Dehler, C. M., Anderson, K., and Nagy, R. M., 2011a, New descriptions of the cap dolostone and associated strata Neoproterozoic Pocatello Formation, southeastern Idaho, U.S.A., *in* Lee, J., and Evans, J. P., eds., Geologic Field Trips to the Basin and Range, Rocky Mountains, Snake River Plain, and Terranes of the U.S. Cordillera: Geological Society of America Field Guide 21: Boulder, Co, Geological Society of America, p. 183-194.

Dehler, C. M., Crossey, L. J., Fletcher, K. E. K., Karlstrom, K. E., Williams, M. L., Jercinovic, M. J., Gehrels, G., Pecha, M., and Heizler, M. T., ChUMP Connection (Chuar-Uinta Mountain-Pahrump): Geochronologic constraints for correlating ca. 750 Ma Neoproterozoic successions of southwestern Laurentia, *in* Proceedings Geologiacl Society of America Abstracts with Programs, Denver, 2011b, Volume 43, p. 55.

Dehler, C. M., Fanning, C. M., Link, P. K., Kingsbury, E. M., and Rybczynski, D., 2010, Maximum depositional age and provenance of the Uinta Mountain Group and Big Cottonwood Formation, northern Utah: Paleogeography of rifting western Laurentia: Geological Society of America Bulletin, v. 122, no. 9/10, p. 1686-1699.

Eisbacher, G. H., 1981, Sedimentary tectonics and glacial record in the Windermere Supergroup, Mackenzie Mountains, northwestern Canada: Geological Survey of Canada Paper 80-27, p. 1-40.

-, 1985, Late Proterozoic rifting, glacial sedimentation, and sedimentary cycles in the light of Windermere deposition, western Canada: Palaeogeography Palaeoclimatology Palaeoecology, v. 51, p. 231-254.

Erwin, D. H., Laflamme, M., Tweedt, S. M., Sperling, E. A., Pisani, D., and Peterson, K. J., 2011, The Cambrian Conundrum: Early Divergence and Later Ecological Success in the Early History of Animals: Science, v. 334, p. 1091-1097.

Evans, D. A. D., 2009, The palaeomagnetically viable long-lived and all-inclusive Rodinia supercontinent reconstruction, *in* Murphy, J. B., Keppie, J. D., and Hynes, A., eds., Ancient Orogens and Modern Analogues, Volume 327: London, Geological Society of London Special Publication, p. 371-404.

Fairchild, I. J., Spiro, B., Herrington, P. M., and Song, T., 2000, Controls on Sr and C isotope compositions of Neoproterozoic Sr-rich limestones of East Greenland and North China, *in* Grotzinger, J. P., and James, N. P., eds., Carbonate Sedimentation and Diagenesis in the Evolving Precambrian World, Volume 67: Tulsa, SEPM Special Publication, p. 297-313.

Fanning, C. M., and Link, P. K., 2004, U-Pb SHRIMP ages of Neoproterozoic (Sturtian) glaciogenic Pocatello Formation: Geology, v. 32, p. 881-884.

Fleck, R. J., 1970, Age and tectonic significance of volcanic rocks, Death Valley area, California: Geological Society of America Bulletin, v. 81, p. 2807-2816.

Goodge, J. W., Vervoort, J. D., Fanning, C. M., Brecke, D. M., Farmer, G. L., Williams, I. S., Myrow, P. M., and DePaulo, D. J., 2008, A positive test of East Antarctica-Laurentia juxtaposition within the Rodinia supercontinent: Science, v. 321, p. 235-240.

Graff, D. A., 1985, Paragenesis of iron formation within the Kingston Peak Formation, southern Death Valley region, California [M.S.: University of California, Davis, 170 p.

Green, O., 2001, A Manual of Practical Laboratory and Field Techniques in Palaeobiology, Dordrecht, Kluwer Academic Publishers, 538 p.:

Gutstadt, A. M., 1968, Petrology and depositional environments of the Beck Spring dolomite (Precambrian), Kingston Range, California: Journal of Sedimentary Petrology, v. 38, p. 1280-1289.

Halverson, G. P., 2006, A Neoproterozoic chronology, *in* Xiao, S., and Kaufman, A. J., eds., Neoproterozoic Geobiology and Paleobiology, Volume Topics in Geobiology 27: New York, NY, Springer, p. 231-271.

Halverson, G. P., Dudás, F. O., Maloof, A. C., and Bowring, S. A., 2007, Evolution of the $^{87}Sr/^{86}Sr$ composition of Neoproterozoic Seawater: Palaeogeography Palaeoclimatology Palaeoecology, v. 256, p. 103-129.

Halverson, G. P., Wade, B. P., Hurtgen, M. T., and Barovich, K. M., 2010, Neoproterozoic Chemostratigraphy: Precambrian Research, v. 182, no. 4, p. 337-350.

Harwood, C. L., and Sumner, D. Y., 2011, Microbialites of the Neoproterozoic Beck Spring Dolomite, Southern California: Sedimentology, v. XX, p. 1-26.

Hazzard, J. C., 1937, Paleozoic section in the Nopah and Resting Springs Mountains, Inyo County, California: California Journal of Mines and Geology, v. 33, no. 4, p. 270-339.

Heaman, L. M., and Grotzinger, J. P., 1992, 1.08 Ga diabase sills in the Pahrump Group, California; implications for development of the Cordilleran Miogeocline: Geology, v. 20, no. 7, p. 637-640.

Hewett, D. F., 1940, New formation names to be used in the Kingston Range, Ivanpah Quadrangle, California: Journal of the Washington Academy of Sciences, v. 30, no. 6, p. 239-240.

-, 1956, Geology and mineral resoures of the Ivanpah Quadrangle, California and Nevada: U.S. Geological Survey Professional paper 275, p. 1-172.

Hildebrand, R. S., 2009, Did westward subduction cause Cretaceous-Tertiary orogeny in the North American Cordillera?: The Geological Society of America, Special Paper 457, p. 1-72.

Hoffman, P. F., 1991, Did the breakout of Laurentia turn Gondwanaland inside-out?: Science, v. 252, no. 5011, p. 1409-1412.

Hoffman, P. F., and Halverson, G. P., 2011, Neoproterozoic glacial record in the Mackenzie Mountains, northern Canadian Cordillera, *in* Arnaud, E., Halverson, G. P., and Shields-Zhou, G., eds., The Geological Record of Neoproterozoic Glaciations, Volume 36: London, The Geological Society, p. 397-412.

Hoffman, P. F., Halverson, G. P., Domack, E. W., Maloof, A. C., Swanson-Hysell, N. L., and Cox, G. M., 2012, Cryogenian glaciations on the southern tropical paleomargin of Laurentia (NE Svalbard and East Greenland), and a primary origin for the upper Russoya (Islay) carbon isotope excursion: Precambrian Research, v. 206-207, p. 137-158.

Hoffman, P. F., Kaufman, A. J., Halverson, G. P., and Schrag, D. P., 1998, A Neoproterozoic Snowball Earth: Science, v. 281, p. 1342-1346.

Hoffman, P. F., and Maloof, A. C., 2003, Comment on: A complex microbiota from snowball Earth times: Microfossils from the Neoproterozoic Kingston Peak Formation, Death Valley, USA, by Corsetti, F.A., Awramik, S.M., and Pierce, D.: Proceedings of the National Academy of Sciences, v. 100, p. 4399-4404.

Hoffman, P. F., and Schrag, D. P., 2002, The snowball Earth hypothesis; testing the limits of global change: Terra Nova, v. 14, no. 3, p. 129-155.

Hoffmann, K. H., Condon, D. J., Bowring, S. A., and Crowley, J. L., 2004, U-Pb zircon date from the Neoproterozoic Ghaub Formation, Namibia: Constraints on Marinoan glaciation: Geology, v. 32, p. 817-820.

James, N. P., Narbonne, G. M., and Kyser, T. K., 2001, Late Neoproterozoic cap carbonates: Mackenzie Mountains, northwestern Canada: precipitation and global glacial meltdown: Canadian Journal of Earth Sciences, v. 38, no. 8, p. 1229-1262.

Jefferson, C. W., and Parrish, R., 1989, Late Proterozoic stratigraphy, U/Pb zircon ages and rift tectonics, Mackenzie Mountains, northwestern Canada: Canadian Journal of Earth Sciences, v. 26, p. 1784-1801.

Karlstrom, K. E., Bowring, S. A., Dehler, C. M., Knoll, A. H., Porter, S. M., DesMarais, D. J., Weil, A. B., Sharp, Z. D., Geissman, J. W., Elrick, M. B., Timmons, J. M., Crossey, L. J., and Davidek, K. L., 2000, Chuar Group of the Grand Canyon: Record of breakup of Rodinia, associated change in the global carbon cycle, and ecosystem expansion by 740 Ma: Geology, v. 28, no. 7, p. 619-622.

Kaufman, A. J., Knoll, A. H., and Narbonne, G. M., 1997, Isotopes, ice ages, and terminal Proterozoic Earth history: Proceedings of the National Academy of Sciences, v. 95, p. 6600-6605.

Keeley, J. A., Link, P. K., Fanning, C. M., and Schmitz, M. D., 2013, Pre- to synglacial rift-related volcanism in the Neoproterozoic (Cryogenian) Pocatello Formation, SE Idaho: New SHRIMP and CA-ID-TIMS constraints: Lithosphere, v. 5, no. 1, p. 128-150.

Kenny, R., and Knauth, P. L., 2001, Stable isotope variations in the Neoproterozoic Beck Spring Dolomite and Mesoproterozoic Mescal Limestone paleokarst: Implications for life on land in the Precambrian: Geological Society of America Bulletin, v. 113, no. 650-658.

Kettler, R. M., 1982, Radioactive mineralization in the conglomerates and pyritic schists of the Kingston Peak Formation, Panamint Mountains, California [M.S. thesis: University of California, 166 p.

Kirschvink, J. L., 1992, Late Proterozoic low-latitude global glaciation: the snowball earth, *in* Schopf, J. W., and Klein, C., eds., The Proterozoic Biosphere: Cambridge, Cambridge University Press, p. 51-52.

Knauth, P. L., and Kennedy, M. J., 2009, The late Precambrian greening of the Earth: Nature, v. 460, p. 728-732.

Knoll, A. H., Javaux, E., Hewitt, D., and Cohen, P. A., 2006, Eukaryotic organisms in Proterozoic oceans: Philosophical Transactions of the Royal Society of London B: Biological Sciences, v. 361, no. 1470, p. 1023-1038.

Labotka, T. C., Albee, A. L., Lanphere, M. A., and McDowell, S. D., 1980, Stratigraphy, structure and metamorphism in the central Panamint Mountains (Telescope Peak quadrangle), Death Valley area, California: Geological Society of America Bulletin, v. 91, p. 843-933.

Li, Z.-X., and Evans, D. A. D., 2011, Late Neoproterozoic 40° intraplate rotation within Australia allows for a tighter-fitting and longer lasting Rodinia: Geology, v. 39, no. 1, p. 39-42.

Li, Z. X., Bogdanova, S. V., Collins, A. S., Davidson, A., De Waele, B., Ernst, R. E., Fitzsimons, I. C. W., Fuck, R. A., Gladkochub, D. P., Jacobs, J., Karlstrom, K. E., Lu, S., Natapov, L. M., Pease, V., Pisarevsky, S. A., Thrane, K., and Vernikovsky, V., 2008, Assembly, configuration, and break-up history of Rodinia: A synthesis: Precambrian Research, v. 160, no. 1-2, p. 179-210.

Licari, G. R., 1978, Biogeology of the late pre-Phanerozoic Beck Spring Dolomite of eastern California: Journal of Paleontology, v. 52, no. 4, p. 767-792.

Link, P. K., Christie-Blick, N., Devlin, W. J., Elston, D. P., Horodyski, R. J., Levy, M., Miller, J. M. G., Pearson, R. C., Prave, A. R., Stewart, J. H., Winston, D., Wright, L. A., and Wrucke, C. T., 1993, Middle and Late Proterozoic stratified rocks of the western U.S. Cordillera, Colorado Plateau, and Basin and Range province, *in* Reed, J. C., Bickford, M. E., Houston, R. S., Link, P. K., Rankin, D. W., Sims, P. K., and Schmus, V., eds., The Geology of North America, Volume C-2, Precambrian: Conterminous U.S.: Boulder, CO, Geological Society of America, p. 463-595.

Love, G. D., Grosjean, E., Stalvies, C., Fike, D. A., Grotzinger, J. P., Bradley, A. S., Kelly, A. E., Bhatia, M., Meredith, W., Snape, C. E., Bowring, S. A., Condon, D. J., and Summons, R. E., 2009, Fossil steroids record the appearance of Demospongiae during the Cryogenian period: Nature, v. 457, p. 718-722.

Lund, K., Aleinikoff, J. N., Evans, K. V., duBray, E. A., DeWitt, E. H., and Unruh, D. M., 2010, SHRIMP U-Pb dating of recurrent Cryogenian and Late Cambrian-Early Ordovician alkalic magmatism in central Idaho: Implications for Rodinian rift tectonics: Geological Society of America Bulletin, v. 122, no. 3/4, p. 430-453.

Lund, K., Aleinikoff, J. N., Evans, K. V., and Fanning, C. M., 2003, SHRIMP geochronology of Neoproterozoic Windermere Supergroup, central Idaho: implications for rifting of western Laurentia and synchroneity of Sturtian glacial deposits: Geological Society of America Bulletin, v. 115, p. 349-372.

Macdonald, F. A., Cohen, P. A., Dudás, F. O., and Schrag, D. P., 2010a, Early Neoproterozoic scale microfossils in the Lower Tindir Group of Alaska and the Yukon Territory: Geology, v. 38, p. 143-146.

Macdonald, F. A., Halverson, G. P., Strauss, J. V., Smith, E. F., Cox, G. M., Sperling, E. A., and Roots, C. F., 2012, Early Neoproterozoic basin formation in the Yukon: Geoscience Canada, v. 39, p. 77-99.

Macdonald, F. A., Schmitz, M. D., Crowley, J. L., Roots, C. F., Jones, D. S., Maloof, A. C., Strauss, J. V., Cohen, P. A., Johnston, D. T., and Schrag, D. P., 2010b, Calibrating the Cryogenian: Science, v. 327, p. 1241-1243.

Macdonald, F. A., Strauss, J. V., Rose, C. V., Dudás, F. O., and Schrag, D. P., 2010c, Stratigraphy of the Port Nolloth Group of Namibia and South Africa and implications for the age of Neoproterozoic iron formations: American Journal of Science, v. 310, p. 862-888.

Macdonald, F. A., Strauss, J. V., Sperling, E. A., Johnston, D. T., Halverson, G. P., Petach, T., Schrag, D. P., Narbonne, G. M., and Higgins, J. A., in press, The stratigraphic relationship between the Shuram carbon isotope excursion, the oxidation of Neoproterozoic oceans, and the first appearance of the Ediacara biota and bilaterian trace fossils in northwestern Canada: Chemical Geology.

MacLean, J. S., Sears, J. W., Chamberlain, K. R., Khudoley, A. K., Prokopiev, A. V., Kropachev, A. P., and Serkina, G. G., 2009, Detrital zircon geochronologic tests of the SE Siberia-SW Laurentia paleocontinental connection: Stephan Mueller Special Publication, v. Series 4, p. 111-116.

Marian, M. L., and Osborne, R. H., 1992, Petrology, petrochemistry, and stromatolites of the middle to late Proterozoic Beck Spring Dolomite, eastern Mojave Desert, California: Canadian Journal of Earth Sciences, v. 29, p. 2595-2609.

Marti-Mus, M., and Moczydlowska, M., 2000, Internal morphology and taphonomic history of the Neoproterozoic vase-shaped microfossils from the Visingso Group, Sweeden: Norsk Geologisk Tidsskrift, v. 80, p. 213-228.

Miller, J. M. G., 1985, Glacial and syntectonic sedimentation: the upper Proterozoic Kinston Peak Formation, southern Panamint Range, eastern California: Geological Society of America Bulletin, v. 96, p. 75-85.

Miller, J. M. G., Troxel, B. W., and Wright, L. A., 1988, Stratigraphy and paleogeography of the Proterozoic Kingston Peak Formation, Death Valley region, eastern California, *in* Gregory, J. L., and Baldwin, E. J., eds., Geology of the Death Valley Region: Santa Ana, CA, South Coast Geological Society, p. 118-142.

Moczydlowska, M., 2008, The Ediacaran microbiota and the survival of Snowball Earth conditions: Precambrian Research, v. 167, p. 1-15.

Moores, E. M., 1991, Southwest US-East Antarctic (SWEAT) connection: a hypothesis: Geology, v. 19, p. 425-428.

Mrofka, D. D., 2010, Competing models for the timing of cryogenian glaciation: Evidence from the Kingston Peak Formation, southeastern California [PhD: University of California at Riverside, 284 p.

Mrofka, D. D., and Kennedy, M. J., 2011, The Kingston Peak Formation in the eastern Death Valley region, *in* Arnaud, E., Halverson, G. P., and Shields-Zhou, G., eds., The Geological Record of Neoproterozoic Glaciations, Volume 36: London, The Geological Society p. 449-458.

Noble, L. F., 1934, Rock Formations of Death Valley, CA: Science, v. 80, no. 2069, p. 173-178.

Ogden, G. G., and Hedley, R. H., 1980, An Atlas of Freshwater Testate Amoebae, Oxford, Oxford University Press, 221 p.:

Olcott, A. N., Sessions, A. L., Corsetti, F. A., Kaufman, A. J., and de Oliviera, T. F., 2005, Biomarker evidence for photosynthesis during Neoproterozoic glaciation: Science, v. 310, no. 5747, p. 471-474.

Peterson, K. J., Cotton, J. A., Gehling, J. G., and Pisani, D., 2008, The Ediacaran emergence of bilaterians: congruence between the genetic and the geological fossils records: Philosophical Transactions of the Royal Society B, v. 363, p. 1435-1443.

Petterson, R., 2009, The basal Ediacaran Noonday Formation, Eastern California, and implications for Laurentian equivalents [PhD: California Insititute of Technology, 225 p.

Petterson, R., Prave, A. R., Wernicke, B. P., and Fallick, A. E., 2011, The Neoproterozoic Noonday Formation, Death Valley region, California: Geological Society of America Bulletin, v. 123, no. 7-8, p. 1317-1336.

Pierce, D., and Cloud, P. E., Jr., 1979, New microbial fossils from ~1.3 billion-year-old rocks of Eastern California: Geomicrobiology Journal, v. 1, no. 3, p. 295-309.

Porter, S., Meisterfeld, R., and Knoll, A. H., 2003, Vase-shaped microfossils from the Neoproterozoic Chuar Group, Grand Canyon: A classification guided by modern testate amoebae: Journal of Paleontology, v. 77, no. 3, p. 409-429.

Porter, S. M., and Knoll, A. H., 2000, Testate amoebae in the Neoproterozoic Era: Evidence from vase-shaped microfossils in the Chuar Group, Grand Canyon: Paleobiology, v. 26, p. 345-370.

Prave, A. R., 1999, Two diamictites, two cap carbonates, two delta 13C excursions, two rifts; the Neoproterozoic Kingston Peak Formation, Death Valley, California: Geology, v. 27, p. 339-342.

Pruss, S. B., Bosak, T., Macdonald, F. A., McLane, M., and Hoffman, P. F., 2010, Microbial facies in a Sturtian cap carbonate, the Rasthof Formation, Otavi Group, northern Namibia: Precambrian Research, v. 181, p. 187-198.

Roberts, M. T., 1982, Depostional environments and tectonic setting of the Crystal Spring Formation, Death Valley region, California, *in* Cooper, J. P., Troxel, B. W., and Wright, L. A., eds., Western Mojave Desert and southern Great Basin, California, Geological Society of America Cordilleran Section meeting guidebood, field trip 9: Shoshone, CA, Death Valley Publishing Company, p. 143-154.

Runnegar, B., 2000, Loophole for snowball Earth: Nature, v. 405, p. 403-404.

Sawaki, Y., Kawai, T., Shibuya, T., Tahata, M., Omori, S., Komiya, T., Yoshida, N., Hirata, T., Ohno, T., Windley, B., and Maruyama, S., 2010, 87Sr/86Sr chemostratigraphy of Neoproterozoic Dalradian carbonates below the Port Askaig Glaciogenic Formation, Scotland: Precambrian Research, v. 179, p. 150-164.

Sears, J. W., 2012, Transforming Siberia along the Laurussian margin: Geology, v. 40, no. 6, p. 535-538.

Sears, J. W., and Price, R. A., 2003, Tightening the Siberian connection to western Laurentia: Geological Society of America Bulletin, v. 115, p. 943-953.

Shields, G., Brasier, M. D., Stille, P., and Dorjnamjaa, D., 2002, Factors contributing to high δ13C values in Cryogenian limestones of western Mongolia: Earth and Planetary Science Letters, v. 196, p. 99-111.

Smith, M. D., Arnaud, E., Arnott, R. W. C., and Ross, G. M., 2011, The record of Neoproterozoic glaciations in the Windermere Supergroup, southern Canadian Cordillera, *in* Arnaud, E., Halverson, G. P., and Shields-Zhou, G., eds., The Geological Record of Neoproterozoic Glaciations, Volume 36: London, Geological Society, p. 413-423.

Snow, J. K., Asmerom, Y., and Lux, D. R., 1991, Permian-Triassic plutonism and tectonics, Death Valley region, California and Nevada: Geology, v. 19, no. 6, p. 629-632.

Snow, J. K., and Wernicke, B. P., 1990, Uniqueness of geological correlations: An example from the Death Valley extended terrain: Geological Society of America Bulletin, v. 101, no. 11, p. 1351-1362.

-, 2000, Cenozoic tectonism in the central Basin and Range: Magnitude, rate, and distribution of upper crustal strain: American Journal of Science, v. 300, p. 659-719.

Stewart, J. H., 1970, Upper Precambrian and Lower Cambrian strata in the southern Great Basin, California and Nevada, U.S. Geological Survey Professional Paper, 206 p.:

Stewart, J. H., 1975, Initial deposits in the Cordilleran geosyncline: Evidence of a late Precambrian (<850 m.y.) continental separation: Geological Society of America Bulletin, v. 83, no. 5, p. 1345-1360.

Strickland, A., Wooden, J. L., Mattinson, C. G., Ushikubo, T., Miller, D. M., and Valley, J. W., 2012, Proterozoic evolution of the Mojave crustal province as preserved in the Ivanpah Mountains, southeastern California: Precambrian Research, v. 224, p. 222-241.

Summa, C. L., 1993, Sedimentologic, stratigraphic, and tectonic controls of a mixed carbonate-siliciclastic succession; Neoproterozoic Johnnie Formation, Southeast California [Ph.D.: Massachusetts Institute of Technology, 615 p.

Thorkelson, D. J., 2000, Geology and mineral occurences of the Slats Creek, Fairchild Lake and "Dolores Creek" areas, Wernecke Mountains, Yukon Territory (106D/16, 106C/13, 106C/14): Exploration and Geological Services Division, Yukon Region, Bulletin 10.

Timmons, M. J., Karlstrom, K. E., Dehler, C. M., Geissman, J. W., and Heizler, M. T., 2001, Proterozoic multistage (~1.1 and ~0.8 Ga) extension in the Grand Canyon Supergroup and establishment of northwest and north-south tectonic grains in the southwestern United States: Geological Society of America Bulletin, v. 113, p. 163-181.

Troxel, B. W., 1966, Sedimentary features of the later Precambrian Kingston Peak Formation Death Valley, California: Geological Society of America Special Paper v. 101, p. 341.

-, 1967, Sedimentary rocks of late Precambrian and Cambrian age in the southern Salt Spring Hills, southeastern Death Valley, California: California Division of Mines and Geology Special Report, v. 92, p. 33-41.

-, 1982, Basin facies (Ibex Formation) of the Noonday Dolomite, souther Saddle Peak Hills, southern Death Valley, California, *in* Cooper, J. D., Troxel, B. W., and Wright, L. A., eds., Geology of selected areas in the San Bernardino Mountains, Western Mojave Desert, and Southern Great Basin, California: Shoshone, Death Valley Publishing Co., p. 43-48.

Tucker, M. E., 1986, Formerly aragonitic limestones associated with tillites in the late Proterozoic of Death Valley, California: Journal of Sedimentary Petrology, v. 56, no. 6, p. 818-830.

Vorob'eva, N. G., Sergeev, V. N., and Knoll, A. H., 2009, Neoproterozoic microfossils from the northeastern margin of the East European platform: Journal of Paleontology, v. 83, no. 2, p. 161-196.

Walker, J. D., Klepacki, D. W., and Burchfield, B. C., 1986, Late Precambrian tectonism in the Kingston Range, southern California: Geology, v. 14, p. 15-18.

Wasserburg, G. J., Wetherill, G. W., and Wright, L. A., 1959, Ages in the Precambrian Terrane of Death Valley, CA: Journal of Geology, v. 67, no. 6, p. 702-708.

Wernicke, B. P., Axen, G. J., and Snow, J. K., 1988, Basin and Range extensional tectonics at the latitude of Las Vegas, Nevada: Geological Society of America Bulletin, v. 100, p. 1738-1757.

Wright, L. A., 1954, Geology of the Alexander Hills area, Inyo and San Bernardino Counties, California: California Division of Mines and Geology, Map Sheet 17.

-, 1968, Talc deposits of the souther Death Valley--Kingston Range region, California: California Division of Mines and Geology Special Report, v. 95, p. 79.

-, 1974, Geology of the southeast quarter of Tecopa Quadrangle, Inyo County, California: Californian Division of Mines and Geology.

-, 1976, Late Cenozoic fault patterns and stress fields in the Great Basin and westward displacement of the Sierra Nevada block: Geology, v. 4, p. 489-494.

Wright, L. A., Thompson, R. A., Troxel, B. W., Pavlis, T. L., DeWitt, E. H., Otton, K., Ellis, M. A., Miller, M. G., and Serpa, L. F., 1991, Cenozoic magmatic and tectonic evolution of the east-central Death Valley region, California, *in* Walawender, M. J., and Hanan, B. B., eds., Geological Excursions in Southern California and Mexico, Field Trip Guidebook: Boulder, CO, Geological Society of America, p. 93-127.

Wright, L. A., and Troxel, B. W., 1984, Geology of the Northern half of the Confidence Hills 15-minute Quadrangle, Death Valley Region, Eastern California: The area of the Amaragosa Chaos: California Division of Mines and Geology.

Wright, L. A., Troxel, B. W., Williams, E. G., Roberts, M. T., and Diehl, P. E., 1974, Precambrian sedimentary environments of the Death Valley region, eastern California, *in* Troxel, B. W., and Wright, L. A., eds., Death Valley Region, California and Nevada, Guidebook: Shoshone, CA, Death Valley Publishing Co., p. 27-36.

Wright, L. A., Williams, E. G., and Cloud, P. E., Jr., 1978, Algal and cryptalgal structures and platform environments of the late pre-Phanerozoic Noonday Dolomite, eastern California: Geological Society of America Bulletin, v. 89, p. 321-333.

Yin, L., Zhu, M., Knoll, A. H., Yuan, X., Zhang, J., and Hu, J., 2007, Doushantuo embryos preserved inside diapause egg cysts: Nature, v. 446, p. 661-663.

Zhou, C., Tucker, R., Xiao, S., Peng, Z., Yuan, X., and Chen, Z., 2004, New constraints on the ages of Neoproterozoic glaciations in south China: Geology, v. 32, p. 437-440.

Figure Captions

Figure 1: Simplified geological map of the Pahrump Group and Noonday Formation in Death Valley. BM = Black Mountains, SS = Southern Ibex Hills (Saratoga Springs), SPH = Saddle Peak Hills, SW = Sperry Wash, NR = Nopah Range, AK = Alexander Hills, KR = Kingston Range, SH = Silurian Hills.

Figure 2: Schematic and composite stratigraphy of the Pahrump Group in the Panamint Mountains, Saddle Peak Hills, and the Kingston Range. Stratigraphy of the Panamint Mountains modified from Petterson et al. (2011). Note that thicknesses are approximate and not from specific measured sections. Colored triangles represent different lithologies from the underlying units.

Figure 3: Geological map of the Saddle Peak Hills. Geology mapped by the Harvard University field geology class, EPS 74, on the Ibex Pass and Saddle Peak Hills 1:24,000 topographic maps with UTM gridlines. Coordinates are marked with crosses.

Figure 4: a) Unconformity surface defining the base of the upper Crystal Spring Formation. Hammer head is just below a sharply defined surface in blue that separates dark purple-grey hornfelsed siliceous mudstones below from overlying brownish-red, unmetamorphosed quartzitic sandstone above. The hornfelsing was a result of metamorphism associated with the intrusion of 1.08 Ga diabasic bodies. The overlying sandstones contain detrital zircons as young as ca. 770 Ma. Hence, that surface represents a ca. 300 Myr time gap. b) Example of patchily developed breccia along the lower Crystal Spring-upper Crystal Spring unconformity surface. This lithology occurs as lenses and channels eroded into the underlying hornfelsed strata. Clast imbrication and coarse-tail grading indicates a transport and sorting prior to deposition. Clasts consist of abundant hornfelsed siliceous mudstones and sandstones, light-colored, laminated and cross-bedded carbonate and siliciclastic rocks, as well as darker-colored igneous clasts, all of which are derived from the underlying lower Crystal Spring Formation.

Figure 5: Chemo- and lithostratigraphy of the Beck Spring Dolomite at Saddle Peak Hills and in the Kingston Range. See Table S1 of the data repository for $\delta^{13}C$ and $\delta^{18}O$ data.

Figure 6: A) Angular unconformity below the Virgin Spring Limestone (blue line) overlying the Beck Spring Dolomite and upper Crystal Spring Formation in the Saddle Peak Hills. Other contacts between map units are marked with solid white lines, and marker beds are dashed. B) Thinly laminated limestone at sharp basal contact of the Virgin Spring Limestone; coin for scale. Note veins along tension gashes that are parallel to fractures. These veins and fractures are related to Neogene extension rooted to the Black Mountains detachment (Wright and Troxel, 1984) and are consistent with significant fluid flow. C) Graded beds in the Virgin Spring Limestone at Virgin Spring Wash. Tan beds are limestone with disseminated silt-sized quartz grains that grade upwards into black limestone micrite. D) Storm bed of calc-arenite grit with rip-up clast in the Virgin Spring Limestone; note, again, the pervasive small-scale veining.

Figure 7: Chemo- and lithostratigraphy of the Virgin Spring Limestone; see Figure 5 for key to symbols and Tables S1 and S2 of the data repository for $\delta^{13}C$ and $\delta^{18}O$ data. Arrows designate the stratigraphic position of microfossil discoveries shown on Figure 11. Filled circles are carbonate carbon isotopes and open circles are oxygen isotopes. Lowest Sr^{87}/Sr^{86} data used in Figure 12 composite shown in red.

Figure 8: Sedimentary features of the Kingston Peak Formation: a) Granitic grit at KP2-KP3a contact in the Saddle Peak Hills. b) Channelized grit at KP3b-KP3c contact in the Saddle Peak Hills. c) Striated clast from KP3 in the Kingston Range. d) Clast of KP3 diamictite within KP4 in the Saddle Peak Hills. e) Beck Spring olistoliths in unit KP3 in the eastern Kinston Range, looking northeast at the southern portion of the Figure 9 map area. Field of view is about 500 m.

Figure 9: Generalized geological map of the oncolite beds in the Kingston Range mapped by Prave and Petterson on the Blackwater Mine and East of Kingston Peak 1:24,000 topographic maps with UTM gridlines. Coordinates are marked with crosses. KP3u =

Upper member, heterolithic facies including fanglomerate, fine to coarse graded-beds (turbidites) and brown to red-brown mudstone; KP3m = Megabreccia member, fanglomerate, brown mudstone and purple-red and yellow-gray shales with dropstones. Blue-colored blocks derived from the Beck Spring Dolomite, dark blue-colored blocks derived from the Crystal Spring Formation, and green colored layers are blocks of the oncolitic- and fossil-bearing Beck Spring unit.

Figure 10: Chemostratigraphy of oncolite bed and olistostromes of the Beck Spring Dolomite. See Figure 5 for key to symbols and Table S1 of the data repository for $\delta^{13}C$ and $\delta^{18}O$ data, including the one point from section R7 that is off scale, presumably due to local remineralization.

Figure 11: SEM images of fossils extracted from the Virgin Spring Limestone at Virgin Spring Wash (A, C, E, F, G)and some possible modern equivalents (B, D). Stratigraphic position of samples shown in Figure 7. A) Possible vase-shaped form (4.1 m from base of section); note smooth exterior and tapering of fossil into aperture. B) Modern testate amoebae, *Nebela spp*. C) Possible microfossil showing cratered surface (5.0 m). D) Modern testate amoebae, *Nebela penardiana*; note scales on surface, creating crater-like appearance. E) Possible vase-shaped fossil (4.3 m). F) Organic microfossil; long filamentous appearances attached to collapsed cup-shaped terminus (4.1 m). G) Organic forms with flat, elongate structure, similar to *Siphonophycus solidum* (5.0 m) (Vorob'eva et al., 2009).

Figure 12: Composite carbonate carbon and strontium isotope chemostratigraphy of the Pahrump Group. Abbreviations used and sources of carbon isotope data: UCS—upper Crystal Spring Formation (Saratoga Springs, Corsetti and Kauffman, 2003); Beck Spr.—Beck Spring Dolomite (Beck Canyon, this paper); VS—Virgin Spring Limestone (Saddle Peak Hills and Virgin Spring Wash, this paper); S—Sourdough limestone (Wildrose Canyon, Petterson et al., 2011); T—Thorndike (South Skidoo, Petterson et al., 2011); 1—Sentinel Peak Member (Southern Nopah Range; Petterson et al., 2011); ND3—Mahogany Flats Member (Eastern Wildrose Canyon Petterson et al., 2011); VSMs—vase shaped mircrofossils; BIF—banded iron formation. Strontium data are color-coded for location. Data tables and references used to construct the strontium composite are in the online data repository, Table S3.

Figure 13: Lithological comparison between a) Oncoids in the upper Beck Spring Dolomite at Beck Canyon in the Kingston Range, and b) the "oncolite bed" in the Kingston Peak Formation of the eastern Kingston Range.

Figure 14: Correlation chart of key Neoproterozoic successions on the western margin of Laurentia. Schematic stratigraphy and age constraints are modified from: 1) This paper; 2) Petterson et al. (2011); 3) Keeley et al. (2013); 4) Dehler et al. (2011a; 2010); 5) Condon & Bowring (2010); 6) Smith et al. (2011); 7) Macdonald et al. (in press); 8) Macdonald et al. (2010a); 9) Thorkelson (2000).

Figure 1

Click here to download Figure: Fig1_Location_map.pdf

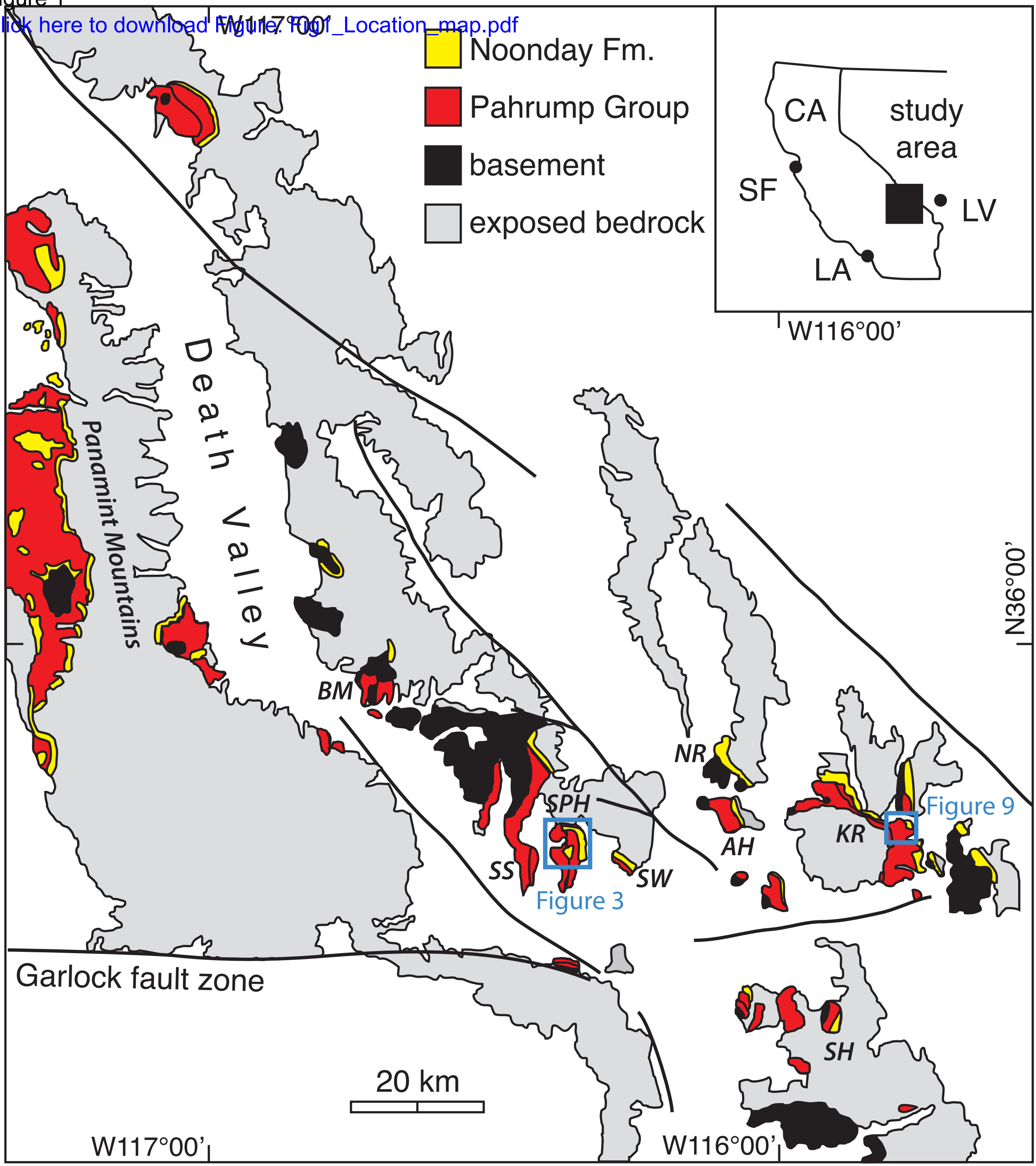

Figure 2

Click here to download Figure: Fig2_schematic_strat.pdf

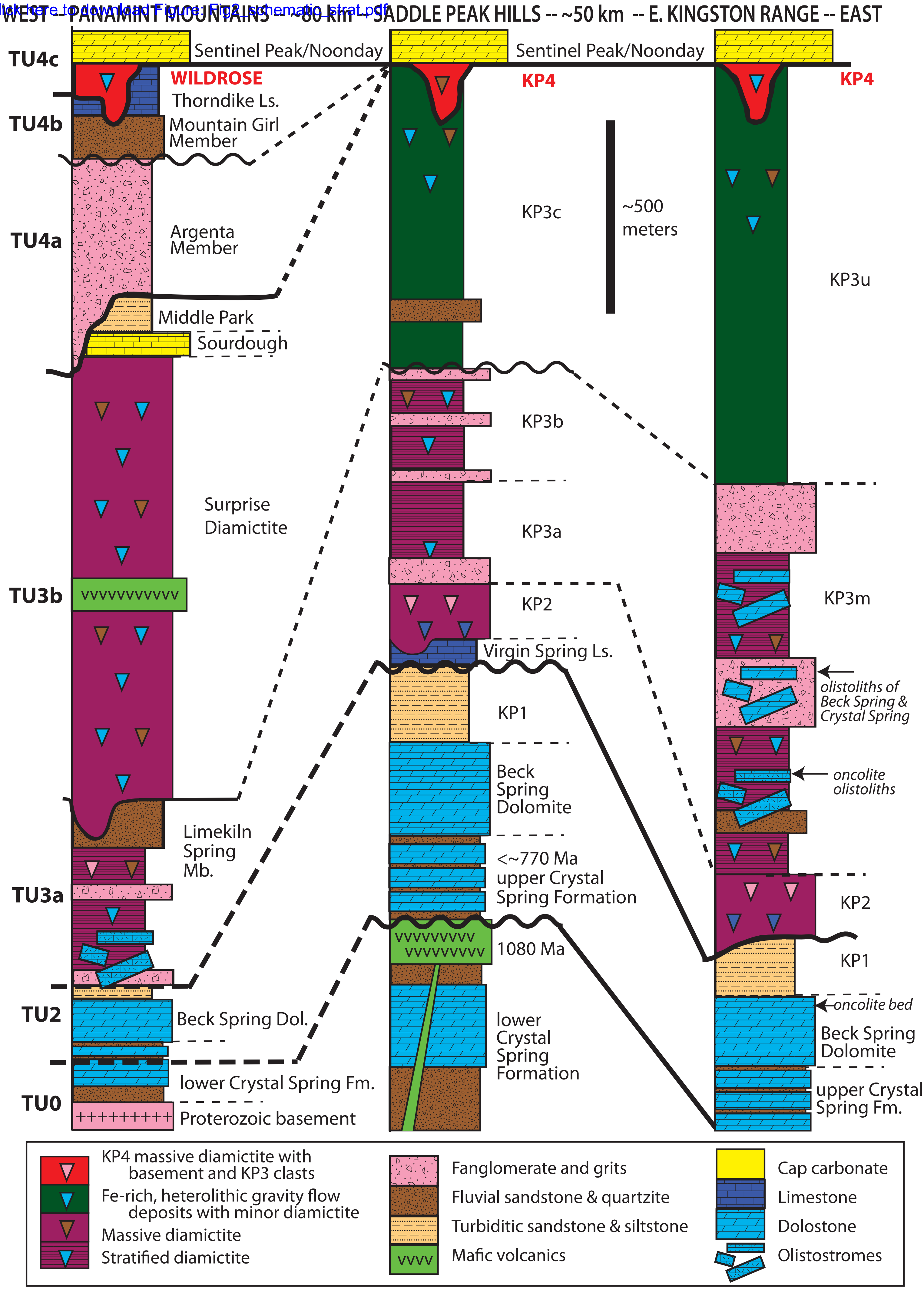

Figure 3

Click here to download Figure: Fig3_SPH_map_V2.pdf

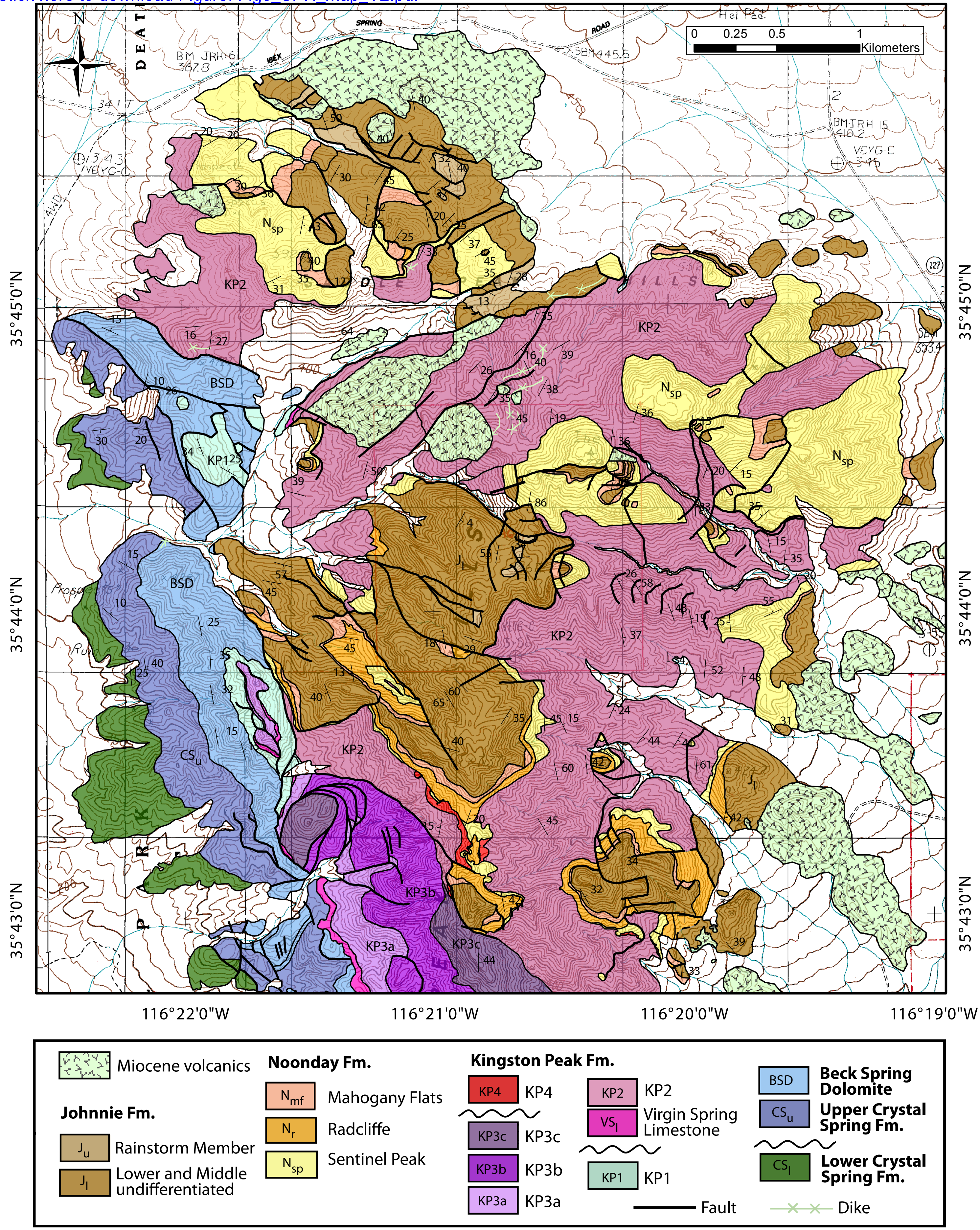

Figure 4
Click here to download high resolution image

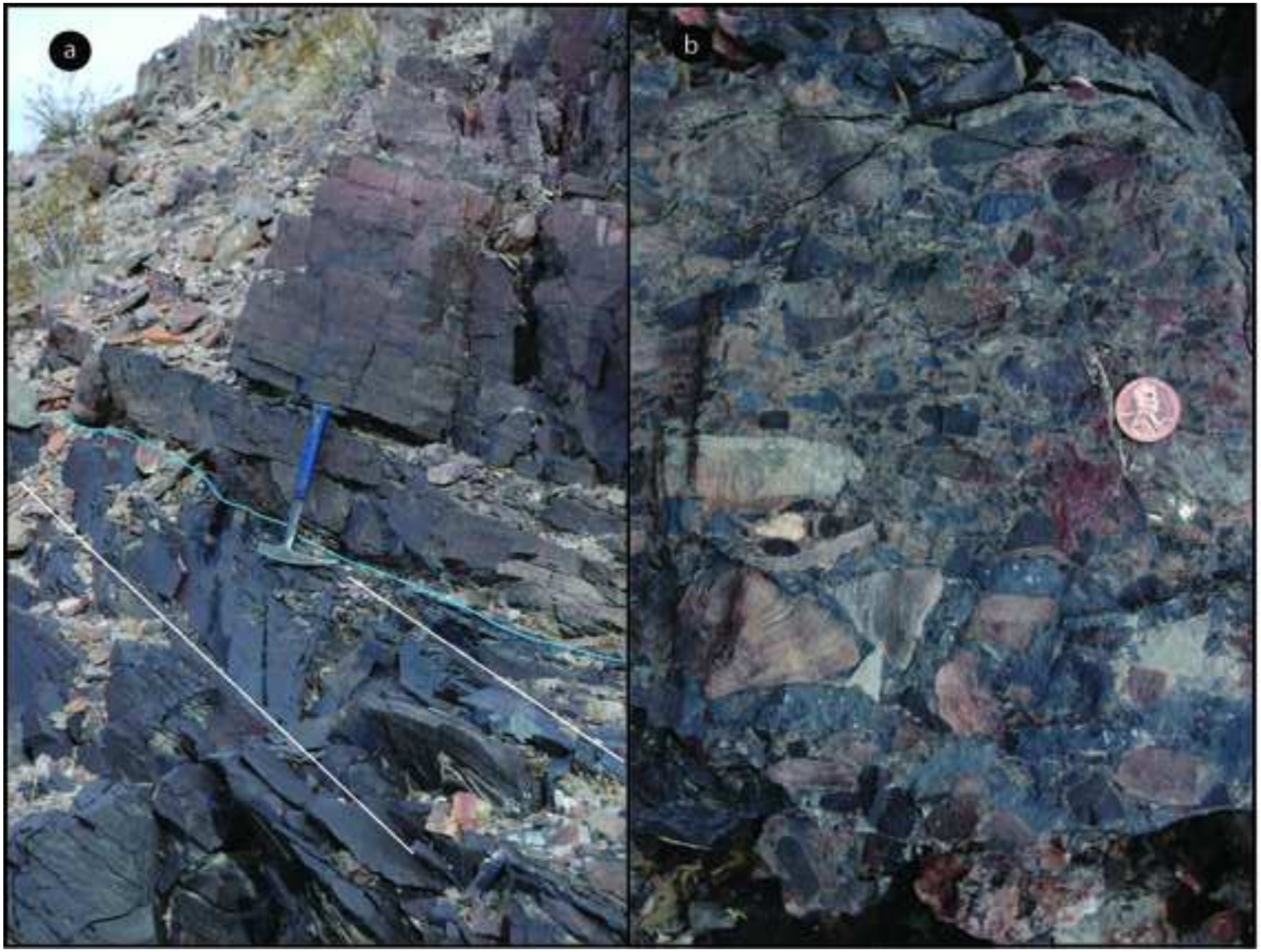

Figure 5

Click here to download Figure: Fig5_BeckSpring_correlation_V5.pdf

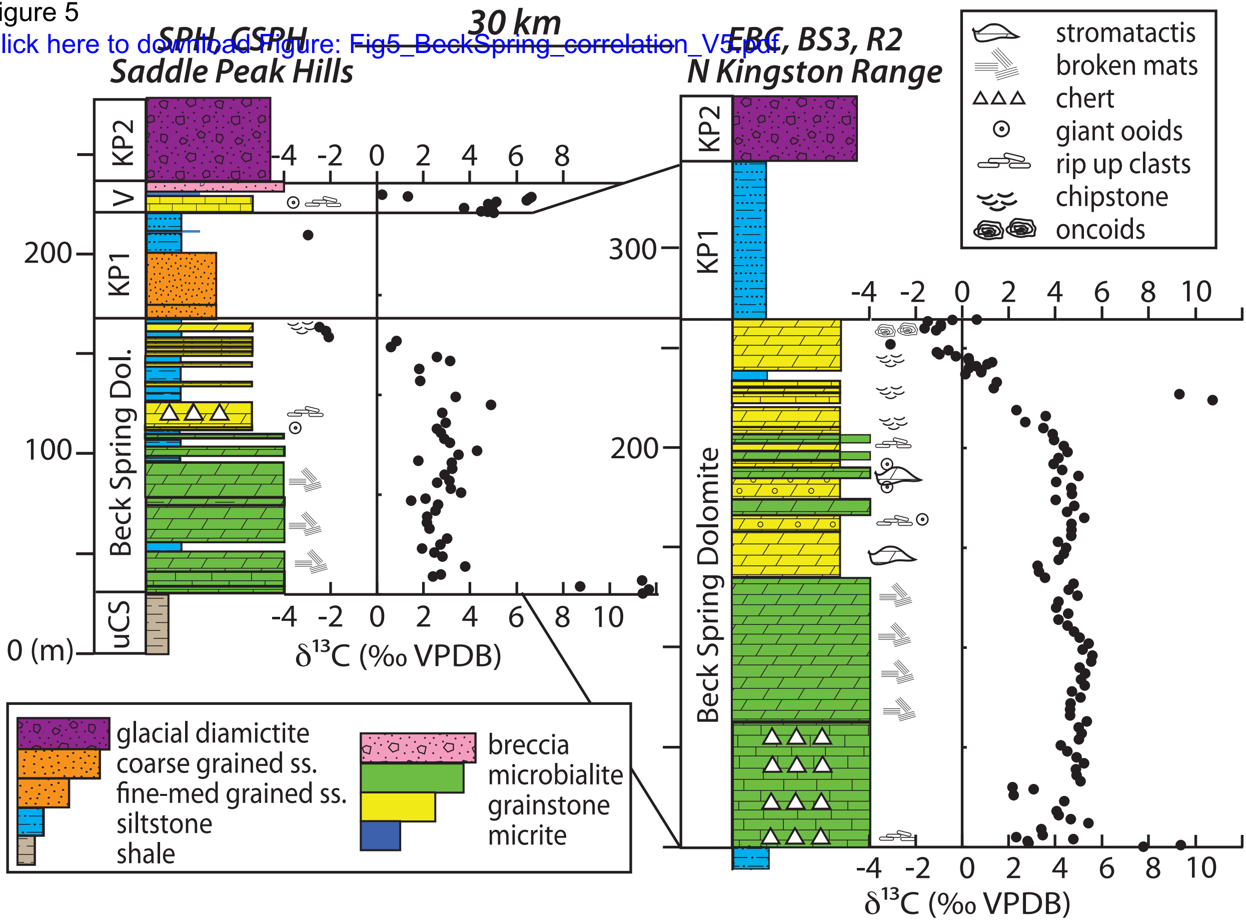

Figure 6
Click here to download high resolution image

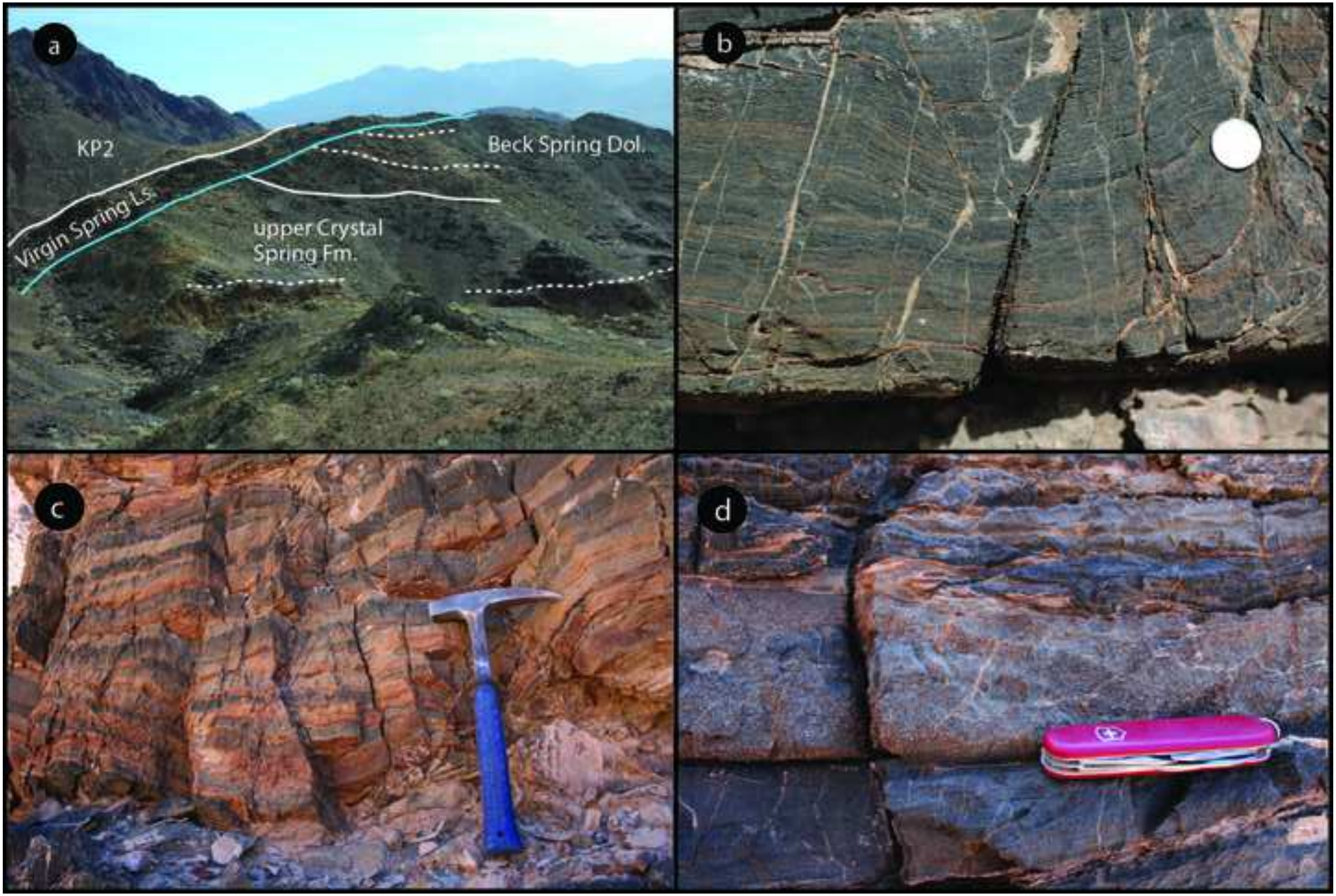

Figure 7

Click here to download Figure Fig7_VSLsections_V2.pdf

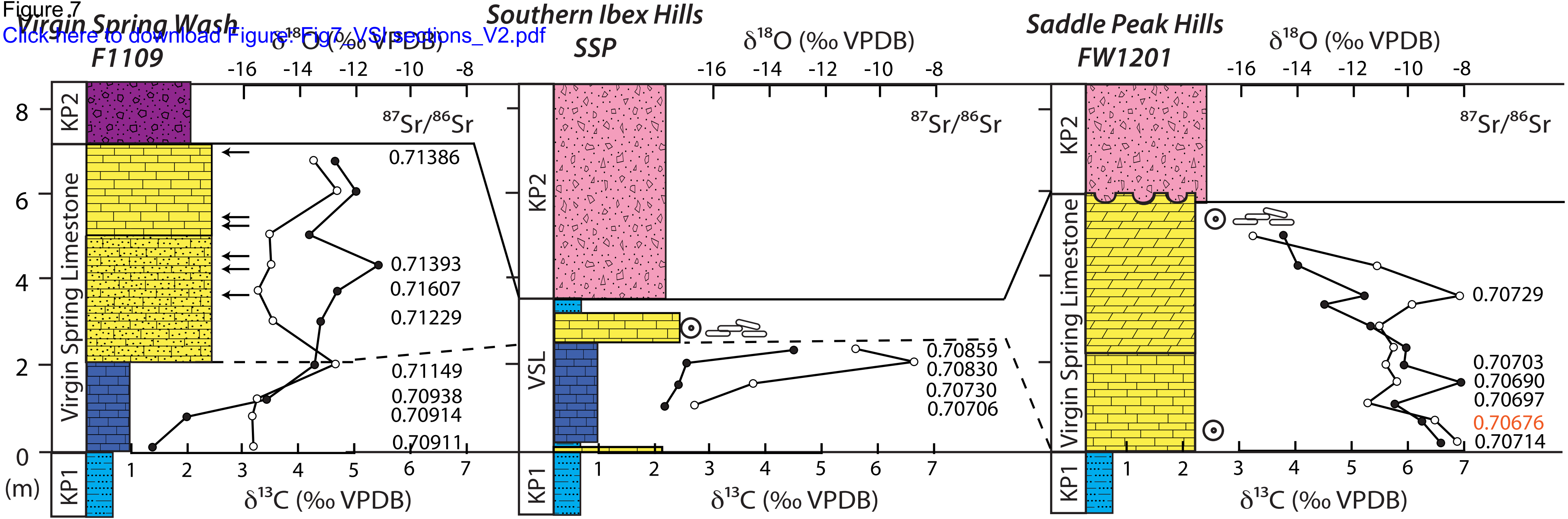

Figure 8

Click here to download high resolution image

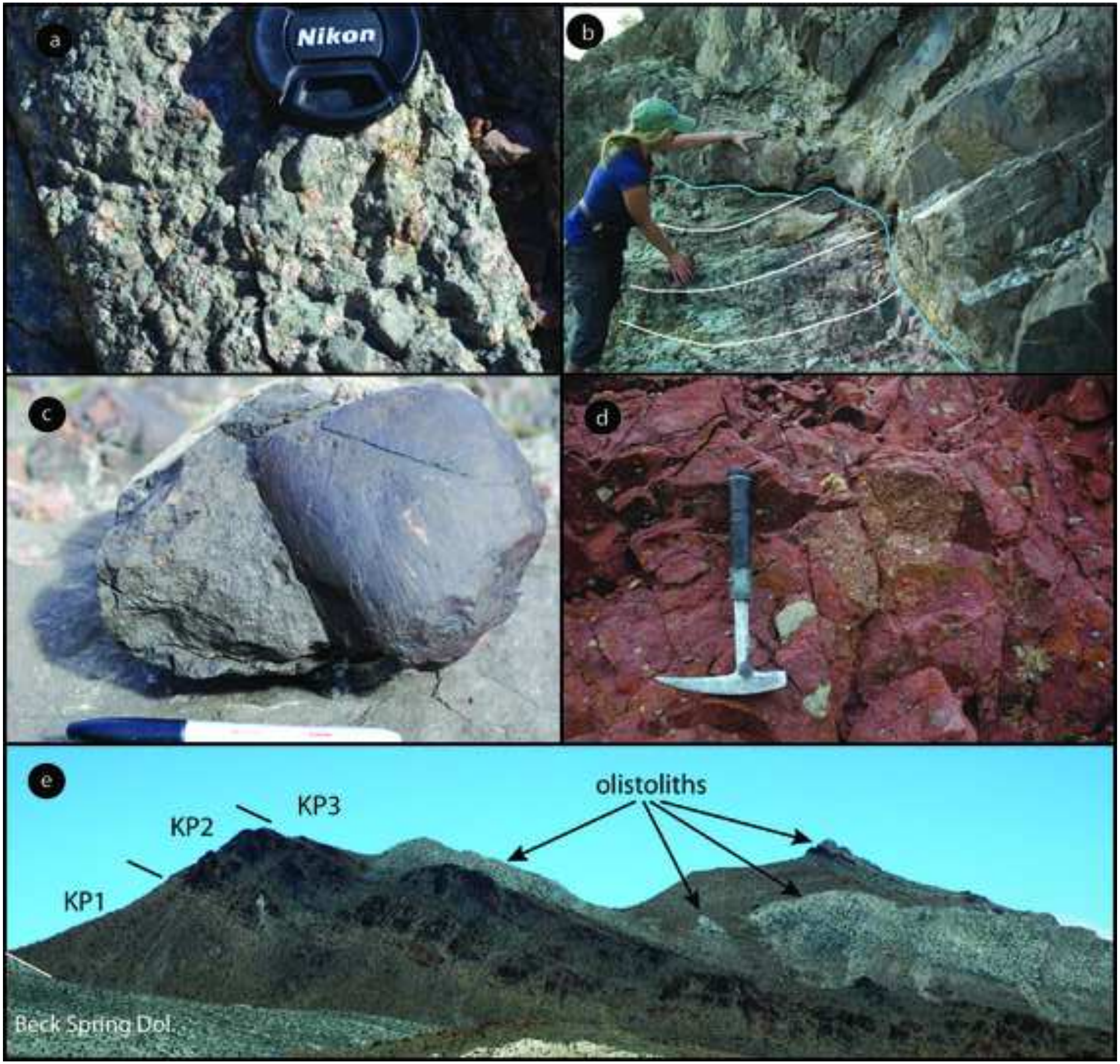

Figure 9

Click here to download Figure: Fig9_OncoliteMap_V3.pdf

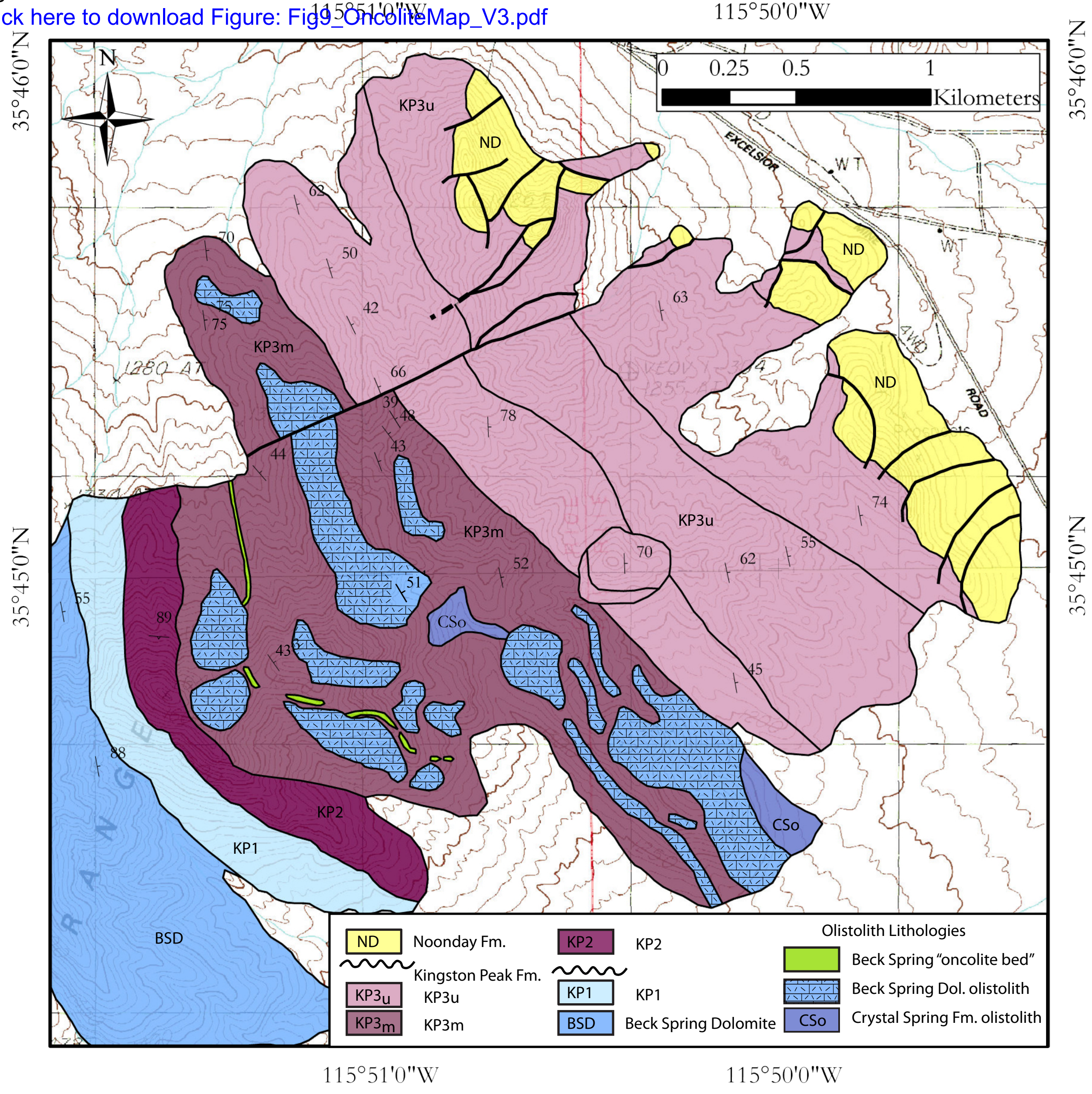

Figure 10

Click here to download Figure: Fig10_olistostrome_bsd_correlation_V2.pdf

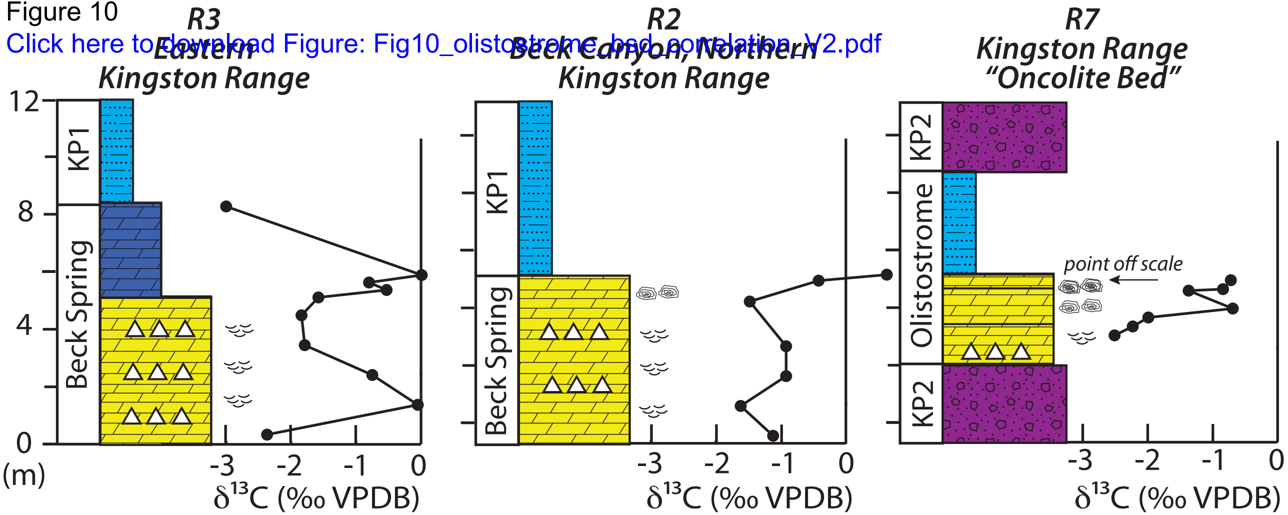

Figure 11
Click here to download high resolution image

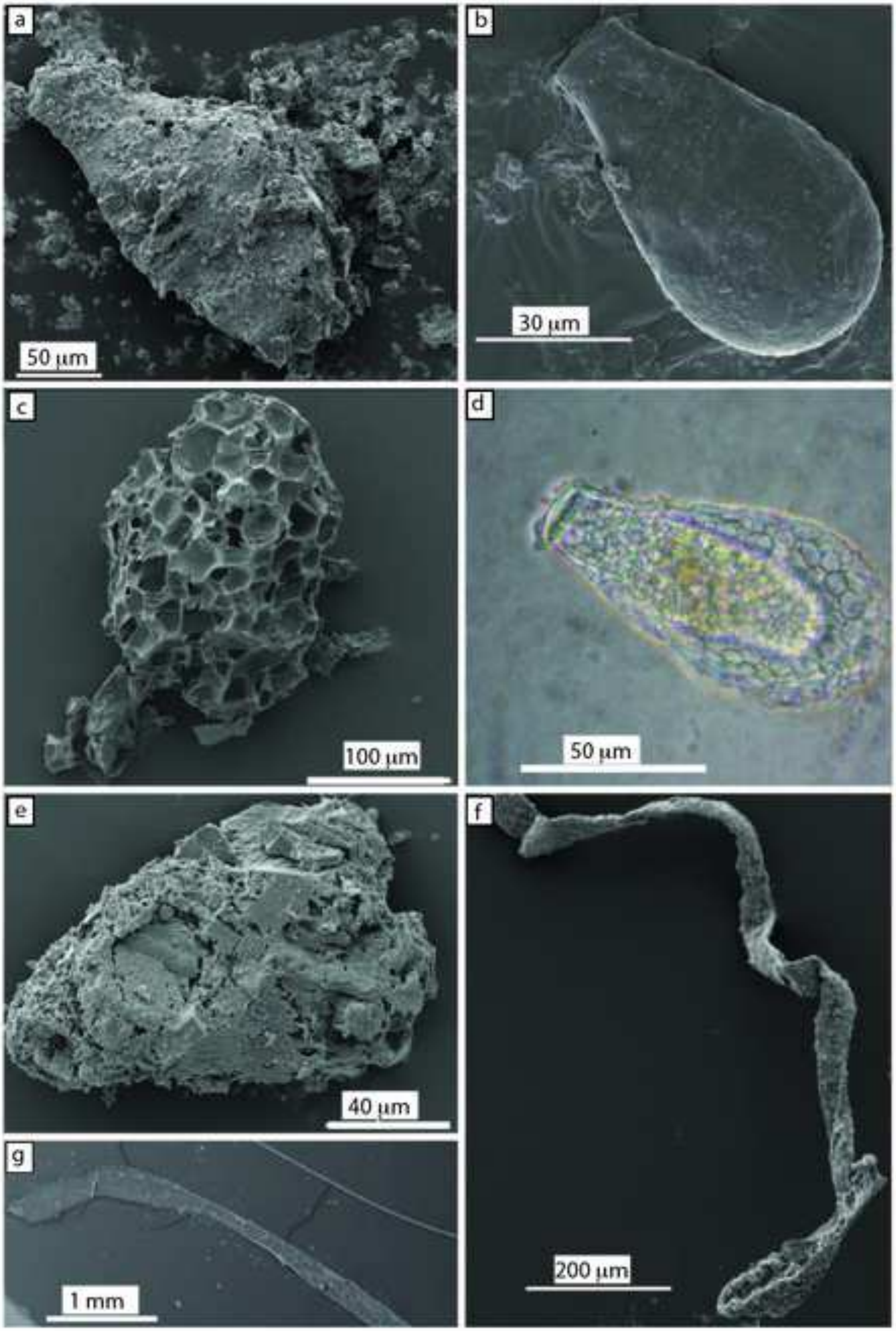

FIGURE 11

Figure 12

Click here to download Figure: Fig12_Composite_V3.pdf

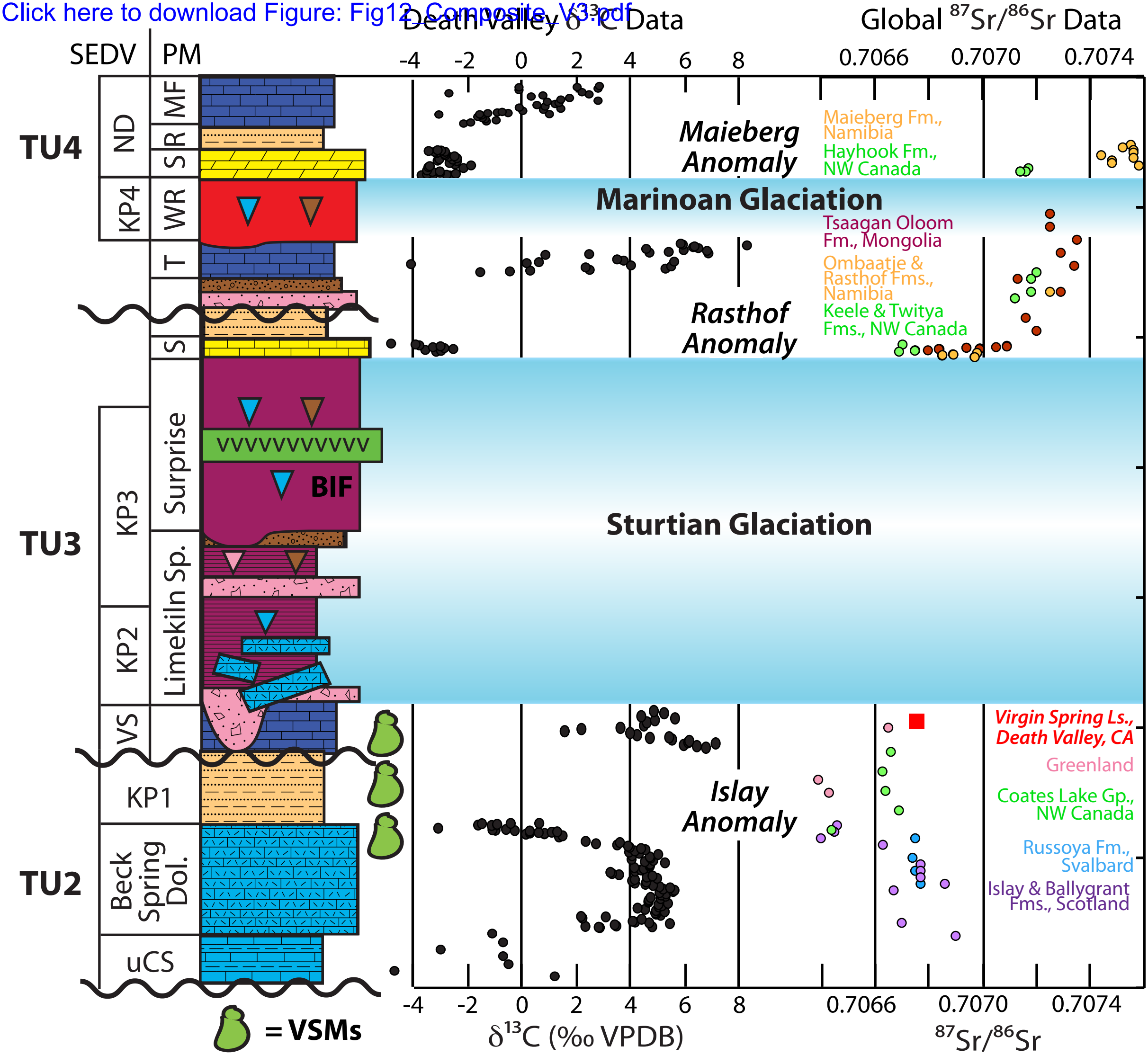

Figure 13
Click here to download high resolution image

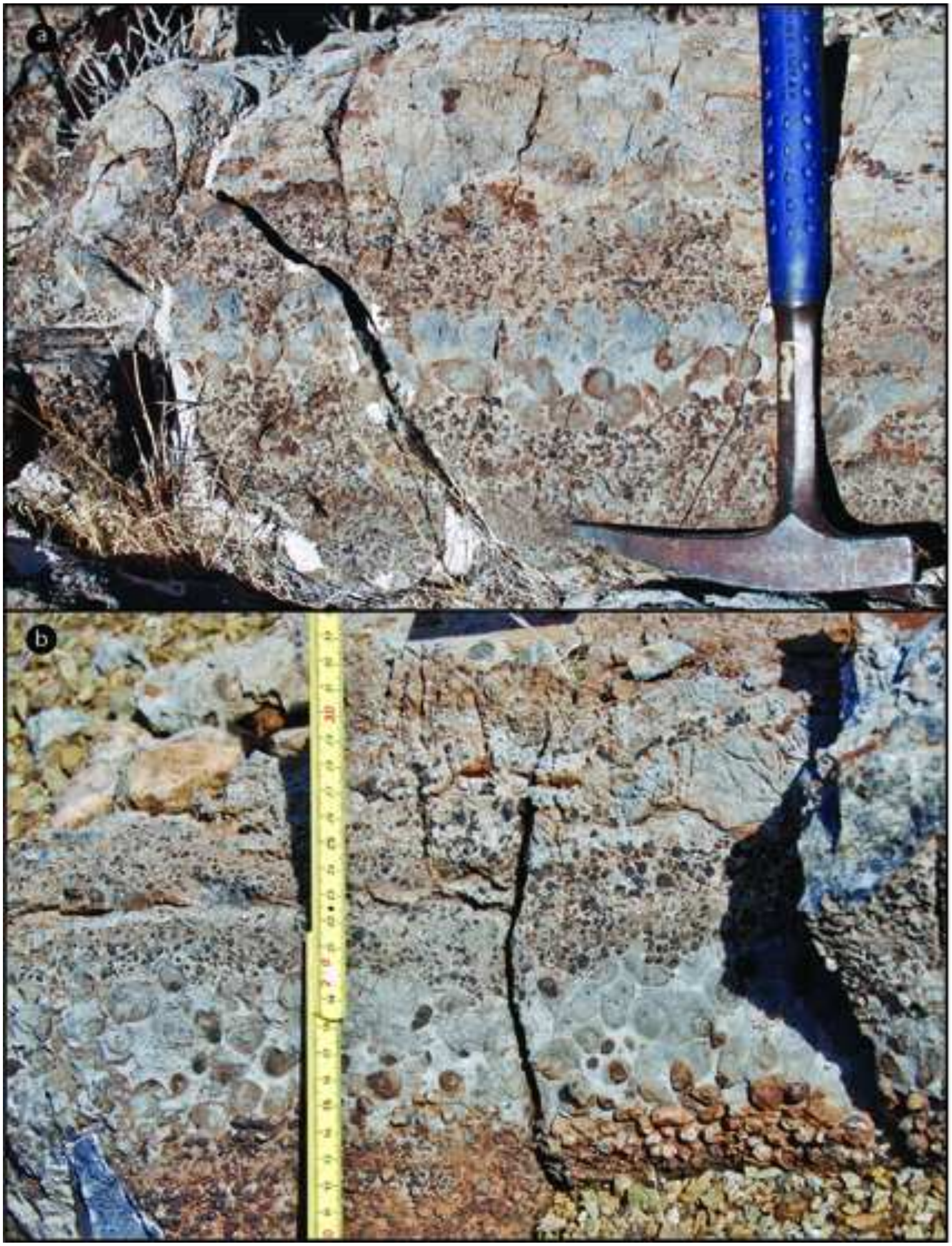

Figure 14

Click here to download Figure: Fig14_WindMnts_Correlation_V2.pdf

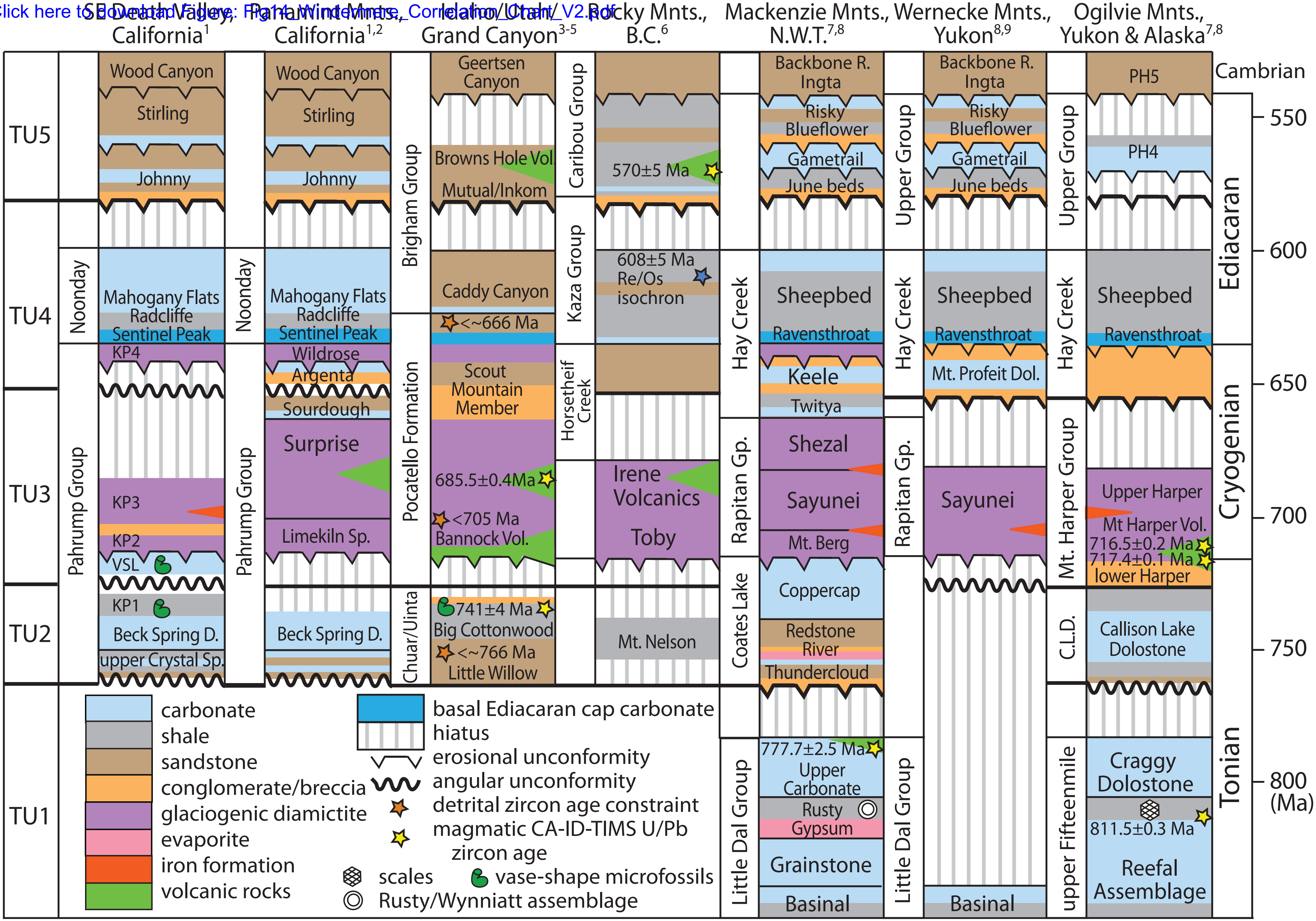

Supplemental file
Click here to download Supplemental file: Table_S1_BeckSpring_COdata.xls

Supplemental file

Click here to download Supplemental file: Table_S2_VirginSpring_COSrTEdata.xls

Supplemental file
Click here to download Supplemental file: Table_S3_Composite_Sr_V2.xls